

DEFORMATION OF A PLATE
WITH CONCENTRATED CORNER SUPPORTS

A THESIS

Presented to
The Faculty of the Graduate Division

by

John Charles Simonis

In Partial Fulfillment
of the Requirements for the Degree
Master of Science in Engineering Mechanics

Georgia Institute of Technology

June 1964

DEFORMATION OF A PLATE
WITH CONCENTRATED CORNER SUPPORTS

Approved:

Chairman

Date approved by Chairman: 5/21/64

TABLE OF CONTENTS

	Page
LIST OF TABLES	iii
LIST OF ILLUSTRATIONS	v
LIST OF SYMBOLS	vi
ACKNOWLEDGEMENTS	vii
SUMMARY	viii
CHAPTER	
I. INTRODUCTION	1
II. THEORETICAL ANALYSIS	5
Trigonometric Solution	8
Polynomial Solution	15
Comparison of Solutions	21
Stresses in a Plate Supported at Four Corners	22
III. DESCRIPTION OF EXPERIMENTAL APPARATUS	25
Test Procedures	32
Data Analysis	37
IV. RESULTS	42
V. CONCLUSIONS	47
Recommendations	48
APPENDIX	49
BIBLIOGRAPHY	98

LIST OF TABLES

Table	Page
1. Set I	43
2. Set II	43
3. Set III	44
4. Set IV	44
5. Experimental Data. Concentrated Load On Diagonals (34 lb). . .	55
6. Experimental Data. Concentrated Load On Diagonals (54 lb). . .	56
7. Experimental Data. Concentrated Load On Center Line	57
8. Experimental Data. Center Load On A Small Area (32 lb)	58
9. Experimental Data. Center Load On A Small Area (48 lb)	59
10. Experimental Data. Center Load On A Small Area (64 lb)	60
11. Experimental Data. Edge Load (80 lb)	61
12. Experimental Data. Edge Load (40 lb)	62
13. Experimental Data. VEE Load	63
14. Experimental Data. Pyramid Load	64
15. Experimental Data. Uniform Load (42 lb)	65
16. Experimental Data. Uniform Load (63 lb)	66
17. Experimental Data. Uniform Load (84 lb)	67
18. Experimental Data. Triangular Load	68
19. Experimental Data. Off Center Concentrated Load Position 4-2 (25 lb)	69
20. Experimental Data. Off Center Concentrated Load Position 4-2 (35 lb)	70
21. Experimental Data. Off Center Concentrated Load Position 4-2 (55 lb)	71

Table		Page
22.	Experimental Data. Concentrated Load Position 3-3 (25 lb)	72
23.	Experimental Data. Concentrated Load Position 3-3 (35 lb)	73
24.	Experimental Data. Concentrated Load Position 3-3 (45 lb)	74
25.	Experimental Data. Concentrated Load Position 3-3 (55 lb)	75
26.	Experimental Data. Outer Loaded Edges (32 lb)	76
27.	Experimental Data. Outer Loaded Edges (48 lb)	77
28.	Experimental Data. Outer Loaded Edges (64 lb)	78

LIST OF ILLUSTRATIONS

Figure	Page
1. Plate Coordinates	7
2. Differential Transformer Detail	27
3. Typical Coil Connection	28
4. Location of Data Points	29
5. Corner Post Detail	30
6. Reference Plate	31
7a. Strain Gage Placement on the Plate Surface	33
7b. Strain Gage Placement on the Plate Surface	34
8. Control Panel	35
9. Loading Frame	36
10. Coil Calibration	39
11a. Evaluation of a Configuration for Five Small Coils	50
11b. Evaluation of a Configuration for Five Small Coils.	51
12. Evaluation of a Configuration for Three Small Coils	52
13a. Evaluation of a Configuration for Two Large Coils Symmetric with Three Small Coils	53
13b. Evaluation of a Configuration for Two Large Coils Symmetric with Three Small Coils	54

LIST OF SYMBOLS

<u>Symbol</u>	<u>Definition</u>
$q(x,y)$	Symmetrical loading function.
x, y, z	Rectangular Coordinates.
$2a, 2b$	Dimensions of the plate.
W	Transverse deflection of the plate.
h	Thickness of the plate.
D	Flexural rigidity of the plate material.
E	Modulus of elasticity.
M_x, M_y, M_{xy}	Bending moments.
Q_x, Q_y	Shear forces.
T	Quantity to obtain true strain.
T	Strain read (Gage factor set)/(factory given gage factor).
V_R	Relative output voltage of differential transformers.
V_T	True output voltage of differential transformers.
U	Potential energy of load displacement.
V	Potential energy of bending.
α, β, γ	Undetermined coefficients of assumed shape function.
ν	Poisson's ratio.
σ_x, σ_y	Maximum principal stresses in respective directions.
τ_{xy}	Maximum shear stress.
ϕ	Angle of rotation of a 60° strain rosette from principle axis.
$\epsilon_a, \epsilon_b, \epsilon_c$	Strain measurement form 60° strain rosette.
$\Theta(x,y)$	Body force loading function.

ACKNOWLEDGMENTS

I am deeply indebted for the financial support given by Georgia Institute of Technology; to Dr. M. E. Raviell and Dr. C. E. Stoneking for their sympathetic encouragement; to Dr. F. M. White for his helpful suggestions; to Dr. F. O. Nottingham, without whose help the experimental electrical systems could not have been constructed; and to all who so unselfishly gave of their time and energy.

SUMMARY

An analysis of a rectangular plate simply supported at four corners with a general symmetric loading has been made using shape functions in the form of trigonometric and polynomial series. The arbitrary parameters of the admissible functions were determined by applying calculus of variations to the total potential energy of the system. Although one cannot guarantee that the derivatives of approximate shape functions will converge to the derivatives of the exact solution, nevertheless differentiation of the approximate shape function was used to obtain the analytic expressions for the stress distributions in the title problem. A general computer program employing the approximate shape functions is presented to determine the deflection and stress distribution. This program is used to analyze the special case of a square plate simply supported at the corners carrying a uniform load.

Experimental analysis was performed to obtain the stresses and deflections in a $30 \times 30 \times 1/4$ in. aluminum plate with various symmetrical and non-symmetrical loadings. The magnitude of the deflections was obtained through the use of differential transformers coupled with the necessary electrical apparatus. Strain measurements were made with strain gages bonded to one surface of the plate.

Extensive experimental data are presented for stress and deflections produced by symmetrical and non-symmetrical loads. Agreement between theoretical and experimental results for symmetrical loads is good. Admissible functions attempting to describe the unsymmetrical loads are not

considered; hence, no comparison can be made between theoretical and experimental results for unsymmetrical loads. However, the experience gained by the comparison of the experimental and theoretical results for symmetrical loads showed the stress and deflection data for unsymmetrical loads to be reasonable.

CHAPTER I

INTRODUCTION

Exact solutions of the biharmonic equation defining the deflection surface of a plate have been established for plates with continuous boundary conditions. However, present technology dictates that reasonably accurate solutions must be found for plates having discontinuous supports along one or more edges, for example: rivets intermittently located along the edge of a plate. To practically satisfy this technological demand one must resort to approximate methods of analysis.

Minimization of the total potential energy by calculus of variations is one of the simplest, yet most powerful, approximate analytical methods in mechanics. Many books devote at least one chapter to the analysis of problems by this method. However, seldom does one find extensions of the basic premise to the "unsolved" problems of today. The limited application of this method can be readily understood when one considers the extensive calculations which must be performed to obtain an answer. The amount of work involved often exceeds the capabilities of some digital computers.

Successful approximate analysis of mechanics problems by the theorem of minimum potential energy requires the inclusion of all predominant energies and exclusion of insignificant energies. In general, the changes in the total potential energy of any elastic system are associated with thermal expansion, torsion, shear, bending, membrane forces, body forces, and loading forces. Thus, one must choose from this

list the effects which suitably describe the system under consideration. A hasty selection of terms can lead to poor analytical results, while the inclusion of secondary effects can lead to extreme complications. An examination of the derivation as well as the significance of each term will allow one to properly formulate the equation of potential energy.

To establish the potential energy for the plate in the title problem, let us assume that we are dealing with a thin, flat, homogeneous, isotropic and elastic plate. Analysis of plate problems, including the particular problem under consideration, using non-linear stress-strain relation is extremely difficult. To circumvent this problem, let us assume a linear stress-strain relation. Furthermore, assume that the lateral deflections (w) are small in comparison to the thickness, thereby allowing the following assumptions of small deflection theory to be used.

1. There is no strain in the middle plane of the plate.
2. Points of the plate lying initially on a normal to the middle plane of the plate remain on the same normal to the middle surface of the plate after bending.
3. The normal stresses in the direction transverse to the plate can be disregarded.

Assumption two immediately eliminates transverse shear force as a possible source of potential energy. Physically this means the shear modulus of the plate is infinite ($G = \infty$). The error caused by neglecting this term becomes appreciable at the edges of thin plates and throughout thick plates. Thus, the approximate energy solutions obtained in the following will be subject to these limitations.

Temperature variations between the upper and lower surfaces of a

plate would result in thermal stresses if the edges of the plate are restrained against rotation and translation. If, linear temperature distributions are assumed, and the plate is simply supported then no thermal stresses will exist.

The von Karman classical plate theory, used in this thesis, neglects the second order and higher order terms in the general equation for strain. This omission destroys the mathematical ability of the derived equation to predict the lateral resistive action of the plate. This omission is justifiable for approximate solutions if the deflections are small in comparison to the thickness (deflections less than half the thickness). Since this is compatible with the original assumptions, the energy due to the stretching of the middle plane will be neglected.

Previous discussions have argued that the energy contributed by thermal expansion, shear, torsion, and stretching of the middle plane is insignificant. However, the potential energy contributed by body forces, loading forces and bending moments cannot be neglected in the formulation of the expression for the total potential energy in a deformed plate. Mathematically this can be expressed as:

$$I = V - U - U_B \quad (1)$$

where

$$V = \frac{D}{2} \int_A \left(\left(\frac{\partial^2 W}{\partial x^2} \right)^2 + \left(\frac{\partial^2 W}{\partial y^2} \right)^2 + 2\nu \frac{\partial^2 W}{\partial x^2} \frac{\partial^2 W}{\partial y^2} + (1-\nu) \left(\frac{\partial^2 W}{\partial x \partial y} \right)^2 \right) dA \quad (2)$$

$$U = \int_A q(x, y) dA \quad (3)$$

$$U_B = \int_A \Theta(x, y) dA \quad (4)$$

If the potential energy contributed by the body forces U_B is considered small in comparison to the potential V and U then equation (1) reduces to:

$$I = V - U \quad (5)$$

Equation (5) lends itself to direct analysis by the theorem of minimum potential energy. This theorem states, "of all displacements satisfying the given boundary conditions, those which satisfy the equilibrium equations make the potential energy a minimum."*

*I. S. Sokolnikoff, Mathematical Theory of Elasticity
McGraw-Hill, 1956, p. 385.

CHAPTER II

THEORETICAL ANALYSIS

Application of the calculus of variations to the minimization of the total potential energy of a system requires the construction of a sequence of minimizing functions

$$\phi_n = C_1 f_1(x) + C_2 f_2(x) + \dots + C_n f_n(x) \quad (6)$$

This sequence must satisfy the geometric boundary conditions of deflection and slope but, not necessarily the natural boundary conditions of moment and shear. Clearly then if one wishes to minimize the integral:

$$I(y) = \int_{x_1}^{x_2} f(x, y, y') dx \quad (7)$$

where $f(x, y, y')$ are continuous and differentiable with respect to y and y' and the derivatives $\partial f / \partial y$ and $\partial f / \partial y'$ are bounded, a sufficient minimization condition is required. This condition exists if it is possible to find any function y which is continuous, has a continuous derivative and satisfies the geometric boundary conditions, and for any $\epsilon > 0$ a finite n and values C_1, C_2, \dots, C_n exist such that with

$$\phi_n = C_1 f_1(x) + C_2 f_2(x) + \dots + C_n f_n(x) \quad (8)$$

the inequalities

$$|\phi - \gamma| < \epsilon$$

$$|\phi'_n - \gamma'| < \epsilon$$

hold for all x in the interval $x_1 < x < x_2$. Then $\lim_{n \rightarrow \infty} I(\phi_n) = I(\gamma_0)$.

The previous discussion has assured the convergence of $I(\phi_n)$ but it has by no means assured that ϕ_n tends to the solution of the original minimum problem, or, that the derivatives of ϕ_n correspond to the derivatives of the original minimum problem. The above discussion is quite pertinent to the theoretical validity of applying calculus of variations to the minimum of the total potential energy. In the practical utilization of this method only a few coordinate functions will enter into the calculations; thus, the theoretical relative completeness of ϕ_n is irrelevant. The initial sequence must be a fair approximation to the actual deflected shape, and the functions $\phi_1, \phi_2 \dots \phi_n$ should be independent so that increasing the number of terms will lead to an actual improvement of the approximation.

The solution of the title problem (see Fig. 1) can be obtained if a functional sequence satisfying the geometric boundary conditions can be constructed. These boundary conditions are:

$$W(\pm a, \pm b) = 0 \quad (9)$$

$$\frac{\partial}{\partial x} W(\pm a, \pm b) \neq 0 \quad (10)$$

$$\frac{\partial}{\partial y} W(\pm a, \pm b) \neq 0 \quad (11)$$

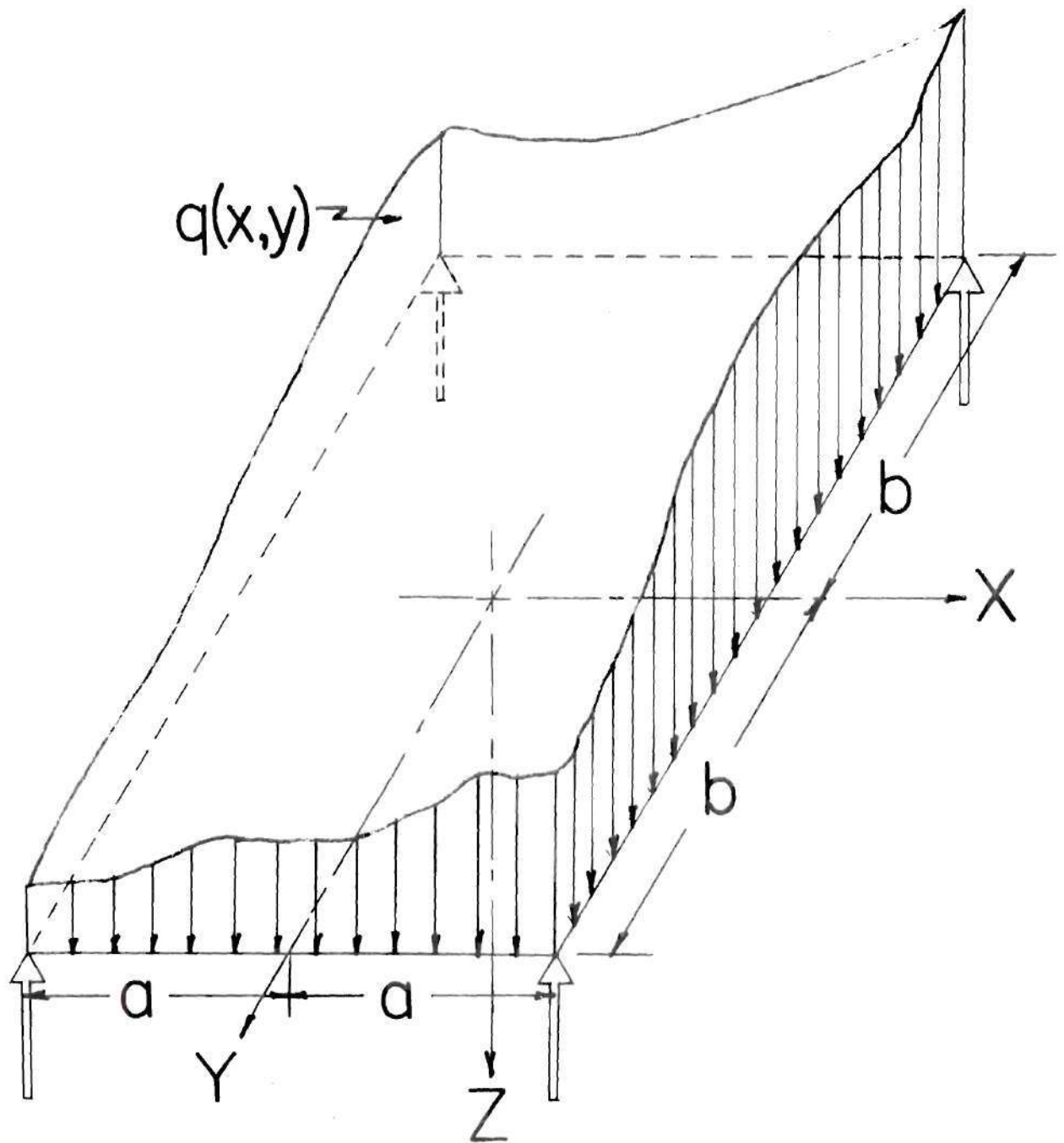


Figure 1. Plate Coordinates.

In addition to the above conditions an admissible function cannot predict, except as specified in equation (9), zero deflection on an exterior boundary of the plate. Furthermore symmetry suggests slope, parallel to the exterior boundaries, must be zero when evaluated at the midpoint of the edge.

Trigonometric Solution

If a coordinate system is associated with the plate as shown in Fig. 1, then a logical assumption for a functional sequence describing symmetric deflection about the coordinate axes is:

$$W = \sum_{m=0}^M \sum_{n=0}^N A_{mn} \cos^n \frac{\pi x}{2a} \cos^m \frac{\pi y}{2b} \quad (12)$$

Immediately one can deduce the slope of the plate to be

$$\frac{\partial W}{\partial x} = - \sum_{m=0}^M \sum_{n=0}^N \frac{n\pi}{2a} A_{mn} \sin^{n-1} \frac{\pi x}{2a} \cos^m \frac{\pi y}{2b} \quad (13)$$

and

$$\frac{\partial W}{\partial y} = - \sum_{m=0}^M \sum_{n=0}^N \frac{n\pi}{2b} A_{mn} \cos^n \frac{\pi x}{2a} \sin^{m-1} \frac{\pi y}{2b} \quad (14)$$

It can be readily verified that the above equations do satisfy the geometric boundary conditions and imposed edge conditions of the physical problem if the constant $A_{00} \equiv 0$.

Although the problem now appears to be straightforward, since a sequence describing the deflection to any desired value of m and n has been found, the deduction of the general formula is an intricate process. Integrals of the form:

$$\int_0^a \int_0^b \left[A_{mn} \frac{m(m-1)\pi^2}{4a^2} \cos \frac{m-2}{2a} x \cos \frac{\pi y}{2b} \right]^2 dx dy \quad (15)$$

must be evaluated. These can be solved, ingeneral, through gamma functions. To simplify the evaluation of the above sequence, it suffices to approximate the deflected shape of the plate using a very limited number of terms.

Four Term Approximation

Equation (12) yields a three parameter shape function if $M = 1$ and $N = 1$, (note $A_{00} \equiv 0$). Summing this equation over these indices yields

$$W = A_{10} \cos \frac{\pi x}{2a} + A_{01} \cos \frac{\pi y}{2b} \quad (16)$$

$$+ A_{11} \cos \frac{\pi x}{2a} \cos \frac{\pi y}{2b}$$

and

$$\frac{\partial W}{\partial X} = -\frac{\pi}{2a} \left\{ A_{10} \sin \frac{\pi X}{2a} + A_{11} \sin \frac{\pi X}{2a} \cos \frac{\pi Y}{2b} \right\} \quad (17)$$

$$\frac{\partial W}{\partial Y} = -\frac{\pi}{2b} \left\{ A_{01} \sin \frac{\pi Y}{2b} + A_{11} \cos \frac{\pi X}{2a} \sin \frac{\pi Y}{2b} \right\} \quad (18)$$

Since the general solution satisfied the geometric and imposed boundary conditions of the system, so also do the above equations. Substitution of equation (15) into equations (2) and (3) of the previous chapter with $\alpha = A_{10}$, $\beta = A_{01}$ and $\gamma = A_{11}$ results in the following equations for potential energy:

$$\begin{aligned} V = & \frac{\pi^4 D}{32} \int_0^a \int_0^b \left[\frac{1}{a^4} \left(\alpha \cos \frac{\pi X}{2a} + \gamma \cos \frac{\pi X}{2a} \cos \frac{\pi Y}{2b} \right)^2 \right. \\ & + \frac{1}{b^4} \left(\beta \cos \frac{\pi Y}{2b} + \gamma \cos \frac{\pi X}{2a} \cos \frac{\pi Y}{2b} \right)^2 \\ & + \frac{2\nu}{a^2 b^2} \left(\alpha \cos \frac{\pi X}{2a} + \gamma \cos \frac{\pi X}{2a} \cos \frac{\pi Y}{2b} \right) \\ & \left. \left(\beta \cos \frac{\pi Y}{2b} + \gamma \cos \frac{\pi X}{2a} \cos \frac{\pi Y}{2b} \right) \right. \\ & \left. + \frac{2(1-\nu)}{a^2 b^2} \gamma^2 \sin^2 \frac{\pi X}{2a} \sin^2 \frac{\pi Y}{2b} \right] dx dy \quad (19) \end{aligned}$$

$$U = \int_0^a \int_0^b q(x, y) \left[\alpha \cos \frac{\pi X}{2a} + \beta \cos \frac{\pi Y}{2b} + \gamma \cos \frac{\pi X}{2a} \cos \frac{\pi Y}{2b} \right]^{(20)} dx dy$$

Substituting equations (19) and (20) into equation (5), of the previous chapter, and minimizing the total energy with respect to the parameters α , β , and γ yield the following conditions:

$$\frac{\partial I}{\partial \alpha} = \frac{\partial}{\partial \alpha} (V - U) \quad (21)$$

$$\frac{\partial I}{\partial \beta} = \frac{\partial}{\partial \beta} (V - U) \quad (22)$$

$$\frac{\partial I}{\partial \gamma} = \frac{\partial}{\partial \gamma} (V - U) \quad (23)$$

Applying these equations to the present values of V and U results in the following three simultaneous linear equations:

$$\frac{b\alpha}{2a^3} + \frac{4\gamma\beta}{\pi^2 ab} + \frac{\gamma}{\pi} \left(\frac{b}{a^3} + \frac{\gamma}{ab} \right) = \frac{16}{\pi^4 D} \int_0^a \int_0^b q(x,y) \cos \frac{\pi x}{2a} dx dy \quad (24)$$

$$\frac{4\gamma\alpha}{\pi^2 ab} + \frac{a\beta}{2b^3} + \frac{\gamma}{\pi} \left(\frac{a}{b^3} + \frac{\gamma}{ab} \right) = \frac{16}{\pi^4 D} \int_0^a \int_0^b q(x,y) \cos \frac{\pi y}{2b} dx dy \quad (25)$$

$$\frac{\alpha}{\pi a} \left(\frac{b}{a^2} + \frac{\gamma}{b} \right) + \frac{\beta}{\pi b} \left(\frac{a}{b^2} + \frac{\gamma}{a} \right) + \frac{\gamma}{4} \left(\frac{a^2 + b^2}{a^3 b^3} \right)^2 = \quad (26)$$

$$\frac{16}{\pi^4 D} \int_0^a \int_0^b q(x,y) \cos \frac{\pi x}{2a} \cos \frac{\pi y}{2b} dx dy$$

The above three equations contain three unknowns. Since an independent set of equations has been obtained, the values for α , β , and γ can be found from these equations. The resulting values of α , β , and γ are:

$$\begin{aligned} \alpha = & \frac{2[\pi^2(a^2+b^2)^2 - 8(a^2+\nu b^2)^2]}{\pi^6 a^2 b^6 D(DEF)} \int_0^a \int_0^b g(x,y) \cos \frac{\pi x}{2a} dx dy \quad (27) \\ & + \frac{16[(b^2+\nu a^2)(a^2+\nu b^2) - \nu(a^2+b^2)^2]}{\pi^6 a^4 b^4 D(DEF)} \int_0^a \int_0^b g(x,y) \cos \frac{\pi y}{2b} dx dy \\ & + \frac{8[8\nu(a^2+\nu b^2) - \pi^2(b^2+\nu a^2)]}{\pi^7 a^2 b^4 D(DEF)} \int_0^a \int_0^b g(x,y) \cos \frac{\pi x}{2a} \cos \frac{\pi y}{2b} dx dy \end{aligned}$$

$$\begin{aligned} \beta = & \frac{16[(a^2+\nu b^2)(b^2+\nu a^2) - \nu(a^2+b^2)^2]}{\pi^6 a^4 b^4 D(DEF)} \int_0^a \int_0^b g(x,y) \cos \frac{\pi x}{2a} dx dy \quad (28) \\ & + \frac{2[\pi^2(a^2+b^2)^2 - 8(b^2+\nu a^2)^2]}{\pi^6 a^6 b^2 D(DEF)} \int_0^a \int_0^b g(x,y) \cos \frac{\pi y}{2b} dx dy \\ & + \frac{8[8\nu(b^2+\nu a^2) - \pi^2(a^2+\nu b^2)]}{\pi^7 a^4 b^2 D(DEF)} \int_0^a \int_0^b g(x,y) \cos \frac{\pi x}{2a} \cos \frac{\pi y}{2b} dx dy \end{aligned}$$

$$\begin{aligned} \gamma = & \frac{8[8\nu(a^2+\nu b^2) - \pi^2(b^2+\nu a^2)]}{\pi^7 a^2 b^4 D(DEF)} \int_0^a \int_0^b g(x,y) \cos \frac{\pi x}{2a} dx dy \quad (29) \\ & + \frac{8[8\nu(b^2+\nu a^2) - \pi^2(a^2+\nu b^2)]}{\pi^7 a^4 b^2 D(DEF)} \int_0^a \int_0^b g(x,y) \cos \frac{\pi y}{2b} dx dy \\ & + \frac{4\pi^4 - 64 - \nu^2}{\pi^8 a^2 b^2 D(DEF)} \int_0^a \int_0^b g(x,y) \cos \frac{\pi x}{2a} \cos \frac{\pi y}{2b} dx dy \end{aligned}$$

where

$$\begin{aligned} \text{DET} = \frac{1}{16\pi^4 a^5 b^5} \{ & \pi^4(a^2+b^2) - 64\nu(a^2+b^2)^2 \\ & + 128\nu(a^2+\nu b^2)(b^2+\nu a^2) - 8\pi^2(a^2+\nu b^2)^2 - 8\pi^2(b^2+\nu a^2)^2 \} \end{aligned} \quad (30)$$

Equations (27) through (30) are quite formidable and do not lend themselves to easy numerical evaluation except through the use of a computer. If one desires a "rough" check on the answers using a three parameter system, a two parameter approximation can be assumed as follows. Let the deflection sequence:

$$W = A_{10} \cos \frac{\pi x}{2a} + A_{01} \cos \frac{\pi y}{2b} \quad (31)$$

Then

$$\frac{\partial W}{\partial x} = -\frac{\pi}{2a} A_{10} \sin \frac{\pi x}{2a} \quad (32)$$

$$\frac{\partial W}{\partial y} = -\frac{\pi}{2b} A_{01} \sin \frac{\pi y}{2b} \quad (33)$$

If the geometric boundary conditions expressed by equation (31) and the intuitive deflection shape of the plate are fulfilled, then one must conclude $A_{00} = 0$. Again using $\alpha = A_{10}$ and $\beta = A_{01}$ we conclude the

approximate deflection sequence to be:

$$W = \alpha \cos \frac{\pi x}{2a} + \beta \cos \frac{\pi y}{2b} \quad (34)$$

Substitution of this equation into equation (2) and (3), of the previous chapter, produces the following equations for potential energy:

$$V = \frac{D}{3} \frac{\pi^4}{2} \int_0^a \int_0^b \alpha^2 \cos^2 \frac{\pi x}{2a} \quad (35)$$

$$+ \frac{\beta^2}{b^2} \cos^2 \frac{\pi y}{2b} + \frac{2\sqrt{2}\beta}{a^2 b^2} \cos \frac{\pi x}{2a} \cos \frac{\pi y}{2b} dx dy$$

and

$$U = \int_0^a \int_0^b q(x,y) [\alpha \cos \frac{\pi x}{2a} + \beta \cos \frac{\pi y}{2b}] dx dy \quad (36)$$

Evaluating equations (21) and (22) in terms of the above potential energies produces the following independent system of simultaneous equations:

$$\frac{b\alpha}{a^3} + \frac{8\sqrt{2}\beta}{\pi^2 ab} = \frac{32}{D\pi^4} \int_0^a \int_0^b q(x,y) \cos \frac{\pi x}{2a} dx dy \quad (37)$$

$$\frac{8\gamma\alpha}{\pi^2 ab} + \frac{a\beta}{b^3} = \frac{32}{D\pi^4} \int_0^a \int_0^b q(x,y) \cos \frac{\pi y}{2b} dx dy \quad (38)$$

The above two equations contain two unknowns α and β . A simultaneous solution for these two parameters yields:

$$\alpha = \frac{\pi^2 a}{b(\pi^4 - 64\gamma^2)} \left\{ \frac{32a^2}{\pi^2 D} \int_0^a \int_0^b q(x,y) \cos \frac{\pi x}{2a} dx dy - \frac{256\gamma b^2}{D\pi^4} \int_0^a \int_0^b q(x,y) \cos \frac{\pi y}{2b} dx dy \right\} \quad (39)$$

$$\beta = \frac{\pi^2 b}{a(\pi^4 - 64\gamma^2)} \left\{ \frac{32b^2}{\pi^2 D} \int_0^a \int_0^b q(x,y) \cos \frac{\pi y}{2b} dx dy - \frac{256\gamma a^2}{D\pi^4} \int_0^a \int_0^b q(x,y) \cos \frac{\pi x}{2a} dx dy \right\} \quad (40)$$

The equations derived for α , β , and γ are valid only for symmetrical loadings. This is "obvious" if one examines the derivatives of (16) (the slopes). It should be noticed from a physical viewpoint that at the midpoint of each side of the plate zero slope exists. Of all the various loading conditions that can be imposed on a plate in general; only symmetrical loadings can produce zero slope at the mid points of each edge of the plate.

Polynomial Solution

A partial check on the manipulations necessary to achieve a solution using a trigonometric shape function is to assume an entirely different

admissible shape function and then compare the coefficients. Trigonometric functions can be approximated uniformly by polynomials in any interval of finite length. The sequence is:

$$W = \sum_{m=0}^M \sum_{n=0}^N A_{mn} \left(1 - \frac{x^2}{a^2}\right)^m \left(1 - \frac{y^2}{b^2}\right)^n \quad (41)$$

Then

$$\frac{\partial W}{\partial x} = \sum_{m=0}^{M-1} \sum_{n=0}^N -\frac{2x}{a^2} (m+1) A_{m+1,n} \left(1 - \frac{x^2}{a^2}\right)^{m+1} \left(1 - \frac{y^2}{b^2}\right)^n \quad (42)$$

$$\frac{\partial W}{\partial y} = \sum_{m=0}^M \sum_{n=0}^{N-1} -\frac{2y}{b^2} (n+1) A_{m,n+1} \left(1 - \frac{x^2}{a^2}\right)^m \left(1 - \frac{y^2}{b^2}\right)^{n+1} \quad (43)$$

One can immediately observe that equation (41) is an admissible functional sequence if the constant term $A_{00} = 0$, and if the geometric boundary conditions described in equation (42) and (43) and the edge conditions imposed by the physical problem are satisfied.

General evaluation of A_{mn} in terms of a general r and s is extremely complicated. In this general solution one obtains integrals of the form:

$$\int_0^a \int_0^b A_{mn} m(m-1) \left(1 - \frac{x^2}{a^2}\right)^{m-2} \left(1 - \frac{y^2}{b^2}\right)^{n-2} dx dy \quad (44)$$

Answers to this type of integral can be conveniently found if the inte-

grand is written in terms of the binomial expansion:

$$\sum_{\epsilon} \binom{n}{\epsilon} x^{n-\epsilon} (-1)^{\epsilon} = (1-x)^n \quad (45)$$

The coefficients n and ϵ are listed in most mathematical tables. It is apparent that an astronomical amount of computation is involved for all but the most conservative expansions of equation (41).

Four Term Polynomial Solution

A pragmatic approach to the use of the deflection sequence described in equation (41) is to let $M = 1$ and $N = 1$. The result of this limited summation is:

$$W = A_{10} \left(1 - \frac{x^2}{a^2}\right) + A_{01} \left(1 - \frac{y^2}{b^2}\right) + A_{11} \left(1 - \frac{x^2}{a^2}\right) \left(1 - \frac{y^2}{b^2}\right) \quad (46)$$

And

$$\frac{\partial W}{\partial x} = -\frac{2x}{a^2} A_{10} - \frac{2x}{a^2} \left(1 - \frac{y^2}{b^2}\right) A_{11} \quad (47)$$

$$\frac{\partial W}{\partial y} = -\frac{2y}{b^2} A_{01} - \frac{2y}{b^2} \left(1 - \frac{x^2}{a^2}\right) A_{11} \quad (48)$$

Since these equations are a direct result of equations (41), (42), and (43), one can immediately conclude that the geometric boundary equations of (46) are fulfilled. If $A_{10} = \alpha$, $A_{01} = \beta$, and $A_{11} = \gamma$ then

$$W = \alpha \left(1 - \frac{x^2}{a^2}\right) + \beta \left(1 - \frac{y^2}{b^2}\right) + \gamma \left(1 - \frac{x^2}{a^2}\right) \left(1 - \frac{y^2}{b^2}\right) \quad (49)$$

By use of the previous equation and equations (2) and (3) for the potential energy one obtains:

$$V = 2D \int_0^a \int_0^b \left(\frac{1}{a^4} [\alpha + \gamma(1 - \frac{y^2}{b^2})]^2 + \frac{2\gamma}{a^2 b^2} [\alpha + \gamma(1 - \frac{y^2}{b^2})][\beta + \gamma(1 - \frac{x^2}{a^2})] \right. \\ \left. + \frac{1}{b^4} [\beta + \gamma(1 - \frac{x^2}{a^2})]^2 + \frac{8(1-\nu)\gamma^2 x^2 y^2}{a^4 b^4} \right) dx dy \quad (50)$$

$$U = \int_0^a \int_0^b g(x,y) [\alpha(1 - \frac{x^2}{a^2}) + \beta(1 - \frac{y^2}{b^2}) + \gamma(1 - \frac{x^2}{a^2})(1 - \frac{y^2}{b^2})] dx dy \quad (51)$$

Minimization of the total potential energy with respect to the parameters α , β , and γ furnishes the following three independent simultaneous equations:

$$b^2 \alpha + \nu a^2 \beta + 2\gamma(\nu a^2 + b^2) = \frac{a^3 b}{4D} \int_0^a \int_0^b g(x,y) (1 - \frac{x^2}{a^2}) dx dy \quad (52)$$

$$\nu b^2 \alpha + a^2 \beta + 2\gamma^3(a^2 + \nu b^2) = \frac{a b^3}{4D} \int_0^a \int_0^b g(x,y) (1 - \frac{y^2}{b^2}) dx dy \quad (53)$$

$$(b^4 + \nu a^2 b^2) \alpha + (a^4 + \nu a^2 b^2) \beta + \frac{4\gamma}{15} (3a^4 + 3b^4 + 5a^2 b^2) = \frac{3 a^3 b^3}{8D} \int_0^a \int_0^b g(x,y) (1 - \frac{x^2}{a^2}) (1 - \frac{y^2}{b^2}) dx dy \quad (54)$$

$$\frac{3 a^3 b^3}{8D} \int_0^a \int_0^b g(x,y) (1 - \frac{x^2}{a^2}) (1 - \frac{y^2}{b^2}) dx dy$$

The solution of this system of equations produces the following result.

$$\gamma = \frac{a^2 b^2}{D(1-\nu)} \left[b^2 (\nu^2 - 1) \int_0^a \int_0^b g(x,y) (1 - \frac{x^2}{a^2}) dx dy + a^2 (\nu^2 - 1) \int_0^a \int_0^b g(x,y) (1 - \frac{y^2}{b^2}) dx dy + (1 - \nu^2) \int_0^a \int_0^b g(x,y) (1 - \frac{x^2}{a^2}) (1 - \frac{y^2}{b^2}) dx dy \right] \quad (55)$$

$$\begin{aligned}
\alpha &= \frac{a^2 b}{30D(DET)} [a^2(a^4 + b^4(6-5\nu^2) + 10a^2b^2(1-\nu)) \int_0^a \int_0^b g(x,y) \left(1 - \frac{x^2}{a^2}\right) dx dy \quad (56) \\
&+ b^2(5a^2b^2 + 5\nu a^2b^2 - \nu b^4 - \nu a^4 + 10\nu a^2b^2) \int_0^a \int_0^b g(x,y) \left(1 - \frac{y^2}{b^2}\right) dx dy \\
&+ \frac{15a^2b^4(\nu^2-1)}{2} \int_0^a \int_0^b g(x,y) \left(1 - \frac{x^2}{a^2}\right) \left(1 - \frac{y^2}{b^2}\right) dx dy] \\
\beta &= \frac{a b^3}{30D(DET)} [a^2(5a^2b^2 - \nu a^4 - \nu b^4 + 5a^2b^2 - 10\nu a^2b^2) \int_0^a \int_0^b g(x,y) \left(1 - \frac{x^2}{a^2}\right) dx dy \quad (57) \\
&+ b^2(b^4 + a^4(6-5\nu^2) + 10a^2b^2(1-\nu)) \int_0^a \int_0^b g(x,y) \left(1 - \frac{y^2}{b^2}\right) dx dy \\
&+ \frac{15a^4b^2(\nu^2-1)}{2} \int_0^a \int_0^b g(x,y) \left(1 - \frac{x^2}{a^2}\right) \left(1 - \frac{y^2}{b^2}\right) dx dy] \\
DET &= \frac{2}{15} (1-\nu^2)a^2b^2 [10a^2b^2(1-\nu) + a^4 + b^4] \quad (58)
\end{aligned}$$

Numerical evaluation of the above equations is a very tedious operation and for this reason it is wise to form a check on our solution. This can be accomplished at least for the first three terms if we choose a deflection sequence of the form:

$$W = \alpha \left(1 - \frac{x^2}{a^2}\right) + \beta \left(1 - \frac{y^2}{b^2}\right) \quad (59)$$

then:

$$\frac{\partial W}{\partial x} = -\frac{2\alpha x}{a^2} \quad (60)$$

$$\frac{\partial W}{\partial y} = -\frac{2\beta y}{b^2} \quad (61)$$

Notice that equation (59) expresses the first two terms of equation (49). Through this similarity equation (59) must be an admissible function and satisfy the appropriate boundary conditions. Substitution of equation (59) must be an admissible function and satisfy the appropriate boundary conditions. Substitution of equation (59) into equations (2) and (3) results in the following equations of potential energy:

$$V = D \int_0^a \int_0^b \left[\frac{2\alpha^2}{a^4} + \frac{2\beta^2}{b^4} + \frac{4\nu\alpha\beta}{a^2b^2} \right] dx dy \quad (62)$$

$$U = \int_0^a \int_0^b g(x,y) \left[\alpha \left(1 - \frac{x^2}{a^2} \right) + \beta \left(1 - \frac{y^2}{b^2} \right) \right] dx dy \quad (63)$$

Minimization of the total potential energy with respect to the parameters α and β determines the following two independent simultaneous equations:

$$b^2\alpha + a^2\nu\beta = \frac{a^3b}{4D} \int_0^a \int_0^b g(x,y) \left(1 - \frac{x^2}{a^2} \right) dx dy \quad (64)$$

$$b^2\nu\alpha + a^2\beta = \frac{ab^3}{4D} \int_0^a \int_0^b g(x,y) \left(1 - \frac{y^2}{b^2} \right) dx dy \quad (65)$$

Solving these equations yields:

$$\alpha = \frac{a}{4bD(1-\nu^2)} \left[\frac{a^2}{\int_0^a \int_0^b g(x,y) \left(1 - \frac{x^2}{a^2} \right) dx dy} - \nu b^2 \int_0^a \int_0^b g(x,y) \left(1 - \frac{y^2}{b^2} \right) dx dy \right] \quad (66)$$

$$\beta = \frac{b}{4aD(1-\nu^2)} \left[b^2 \int_0^a \int_0^b q(x,y) \left(1 - \frac{y^2}{b^2}\right) dx dy - \nu a^2 \int_0^a \int_0^b q(x,y) \left(1 - \frac{x^2}{a^2}\right) dx dy \right] \quad (67)$$

The parameters α , β , and γ derived for a sequence of polynomials contain a hidden limitation. The loading function $q(x, y)$ contained in each equation must be symmetrical. This can be verified through the derivatives of our deflection sequence. These derivatives predict zero slope at the mid point of each side. The only loading condition which will deflect the plate such that zero slope occurs at the center of each edge is a symmetrical one.

Comparison of Solutions

The "best" coefficients for the two and three parameter trigonometric and polynomial deflection sequences have been determined. By careful inspection one immediately notes similarities in the solutions for α , β , and γ . This is quite apparent in the two parameter solutions, for here one can readily see the magnitude of the terms that make the trigonometric and polynomial solutions slightly different. Evaluations of α , β , and γ for a square plate presented on page 81 and 82 are similar in numerical value. An approximate check has been found for the numerical manipulation involved in the three parameter solutions. The solutions presented thus far are a good approximation to the values presented by Timoshenko in the Theory of Plates and Shells on page 220. It is emphasized that the solutions are applicable only to symmetrically loaded plates.

Stresses in a Plate Supported at Four Corners

If the middle surface of a thin plate is bent with small deflection, i.e., deflections small in comparison to the thickness, the following assumptions can be made:

1. Planes before bending remain planes after bending.
2. The middle plane of the plate contains the neutral surface.
3. The stress in the Z direction, see Fig. 1, is small compared to the other stress components and may be neglected in the stress-strain relationships.
4. The theorems and assumptions developed in linear elasticity are applicable.

Application of these equations to an infinitesimal element of the plate yields:

$$M_x = D \left(\frac{\partial^2 W}{\partial x^2} + \nu \frac{\partial^2 W}{\partial y^2} \right) \quad (68)$$

$$M_y = D \left(\frac{\partial^2 W}{\partial y^2} + \nu \frac{\partial^2 W}{\partial x^2} \right) \quad (69)$$

$$M_{xy} = D (1 - \nu) \frac{\partial^2 W}{\partial x \partial y} \quad (70)$$

$$Q_x = -D \left(\frac{\partial^3 W}{\partial x^3} + \frac{\partial^3 W}{\partial x \partial y^2} \right) \quad (71)$$

$$Q_y = -D \left(\frac{\partial^3 W}{\partial y \partial x^2} + \frac{\partial^3 W}{\partial y^3} \right) \quad (72)$$

$$\sigma_{xMAX} = \frac{6 M_x}{h^2} \quad (73) \quad \sigma_{yMAX} = \frac{6 M_y}{h^2} \quad (74)$$

Evaluation of equations (68) through (74) can be accomplished through the use of the deflection sequence described by equations (12) and (41). Since the three parameter sequences, equations (31) and (59), are a special case of the four parameter sequences, where $A_{\infty} = 0$, we can form the following equations for moments, shears, and stresses.

The equations for moments, shears, and stresses for the trigonometric deflection sequence are:

$$M_x = \frac{\pi^2 D}{4a^2 b^2} \left[\alpha b^2 \cos \frac{\pi x}{2a} + \beta \nu a^2 \cos \frac{\pi y}{2b} + \gamma (\nu a^2 + b^2) \cos \frac{\pi x}{2a} \cos \frac{\pi y}{2b} \right] \quad (75)$$

$$M_y = \frac{\pi^2 D}{4a^2 b^2} \left[\alpha b^2 \nu \cos \frac{\pi x}{2a} + \beta a^2 \cos \frac{\pi y}{2b} + \gamma (a^2 + \nu b^2) \cos \frac{\pi x}{2b} \cos \frac{\pi y}{2b} \right] \quad (76)$$

$$Q_x = -\frac{\pi^3 D}{8a^3 b^2} \sin \frac{\pi x}{2a} \left[\alpha b^2 + \gamma (a^2 + b^2) \cos \frac{\pi y}{2b} \right] \quad (77)$$

$$Q_y = -\frac{\pi^3 D}{8a^2 b^3} \sin \frac{\pi y}{2b} \left[\beta a^2 + \gamma (a^2 + b^2) \cos \frac{\pi x}{2a} \right] \quad (78)$$

$$\sigma_x = \frac{3\pi^2 D}{2a^2 b^2 h^2} \left[\alpha b^2 \cos \frac{\pi x}{2a} + \beta \nu a^2 \cos \frac{\pi y}{2b} + \gamma b^2 + \nu a^2 \cos \frac{\pi x}{2a} \cos \frac{\pi y}{2b} \right] \quad (79)$$

$$\sigma_y = \frac{3\pi^2 D}{2a^2 b^2 h^2} \left[\alpha \nu b^2 \cos \frac{\pi x}{2a} + \beta a^2 \cos \frac{\pi y}{2b} + \gamma (a^2 + \nu b^2) \cos \frac{\pi x}{2a} \cos \frac{\pi y}{2b} \right] \quad (80)$$

The equations for the moments, shears, and stresses predicted by

the polynomial deflection functions are:

$$M_x = \frac{2D}{a^2 b^2} [\alpha b^2 + \beta v a^2 + \gamma [(b^2 - y^2) + v(a^2 - x^2)]] \quad (81)$$

$$M_y = \frac{2D}{a^2 b^2} [\alpha v b^2 + \beta a^2 + \gamma [v(b^2 - y^2) + (a^2 - x^2)]] \quad (82)$$

$$M_{xy} = \frac{4D}{a^2 b^2} \frac{\gamma(1-v)xy}{1} \quad (83)$$

$$Q_x = -\frac{4D}{a^2 b^2} \gamma x \quad (84)$$

$$Q_y = -\frac{4D}{a^2 b^2} \gamma y \quad (85)$$

$$\tau_x = \frac{12D}{a^2 b^2 h^2} [\alpha b^2 + \beta v a^2 + \gamma [(b^2 - y^2) + v(a^2 - x^2)]] \quad (86)$$

$$\tau_y = \frac{12D}{a^2 b^2 h^2} [\alpha v b^2 + \beta a^2 + \gamma [v(b^2 - y^2) + (a^2 - x^2)]] \quad (87)$$

Numerical evaluation of equations (75) through (80) is accomplished by the use of equations (27), (28), and (29) or (39), (40) and for $\gamma = 0$. In a similar manner the values of equations (81) through (87) can be found if the values for α , β , and γ , found in equations (55), (56), and (57) or (66), (67), and for $\gamma = 0$ are known.

CHAPTER III

DESCRIPTION OF EXPERIMENTAL APPARATUS

Various experimental methods used by other investigators to measure deflection have been reported in the scientific literature. These methods can be cataloged into two classifications:

1. Shadows of the deflected plate are projected on a calibrated screen and the deflections measured relative to a zero position.
2. Dial indicators are rigidly supported under the plate to measure relative deflections.

These methods have produced experimental results in agreement with various analytical solutions. However, they appear to be clumsy and not adaptable to methods of rapid data gathering.

The criterion of rapid assembly of data hinted at the need for some type of electrical system. This suggested differential transformers which have been used to measure relative distance on industrial machines but have not been applied to the problem of measuring relative deflection of plates.

Differential transformers consist of three windings and a movable ferro-magnetic core. The two primary windings are excited through an A-C power supply. The secondary winding is arranged symmetrically with respect to the primary, and all windings are coaxial with respect to the movable core. If the core is at the mid position, null point, with respect to the secondaries, connected in series, the voltage induced will be zero. A displacement of the core away from the null point causes a voltage to be induced in the secondaries. The induced voltage is symmetrical

with respect to the null point. This voltage can be measured by a sensitive A-C voltmeter or passed through an A-C amplifier and discriminator circuit to produce a very stable D-C voltage, provided the A-C input voltage remains relatively constant.

The differential transformers used in this experiment were made from surplus relays. Various configurations of the relay coils available were made and tested with cold rolled steel centers operating at a frequency which gave zero phase shift. The results of extensive configuration tests are presented through the graphs on page 55 to 78 of the appendix. The small coils refer to G. E. relay coils CR 2791-B 106 J3 and large coils refer to G. E. relay coils CR 2791-D 101 F3. From these graphs one can observe the best coil configuration to be the assemblage of three small and two large coils as shown in Fig. 2. This configuration was found by experiment to be insensitive to any ferro magnetic material in its immediate exterior surroundings and thus, eliminated the need for any shielding.

The wiring diagram for the 21 differential transformers considered necessary to measure the deflection of the 30 by 30 inch 3031T6 aluminum plate is shown in Fig. 3. To simplify and maintain accurate placement of the differential transforms, a system of grid lines was scribed on the plate as shown in Fig. 4.

Corner posts machined as shown in Fig. 5 were bolted to the reference plate shown in Fig. 6. Small punch marks were made in the corner of the plate as shown in Fig. 4 for alignment and accurate placement of the plate. The plate was then leveled and adjusted to the desired height by the adjustable support at the corner posts.

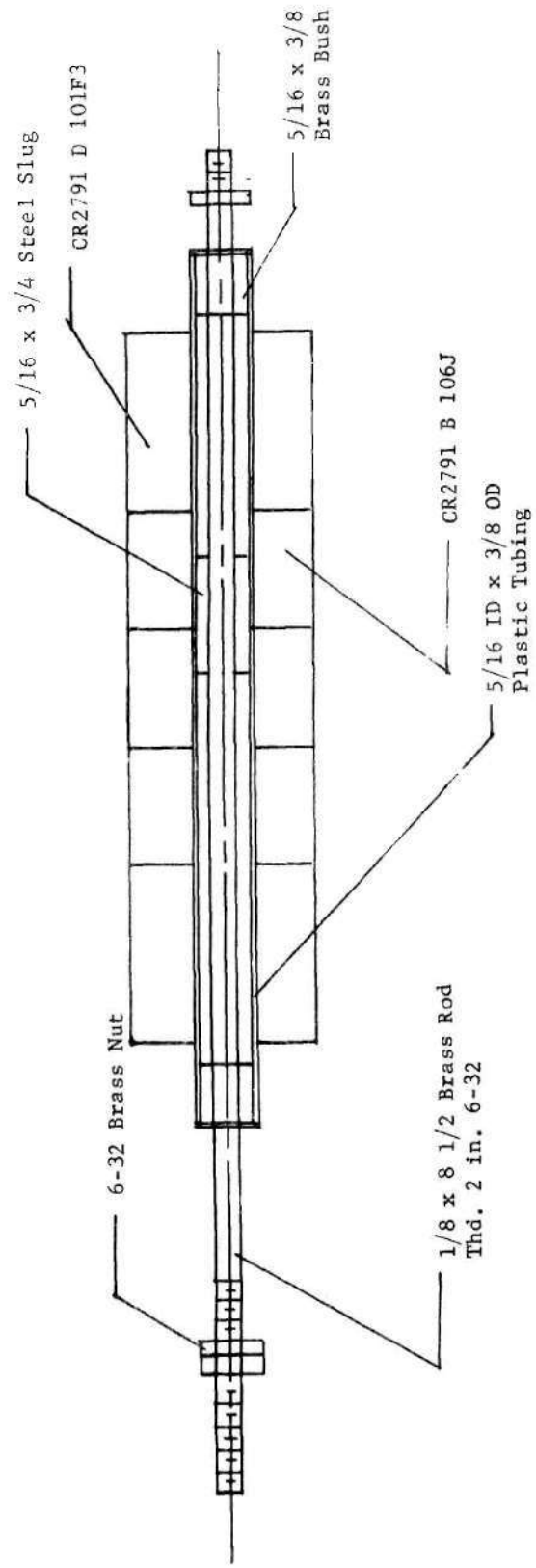


Figure 2. Differential Transformer Detail.

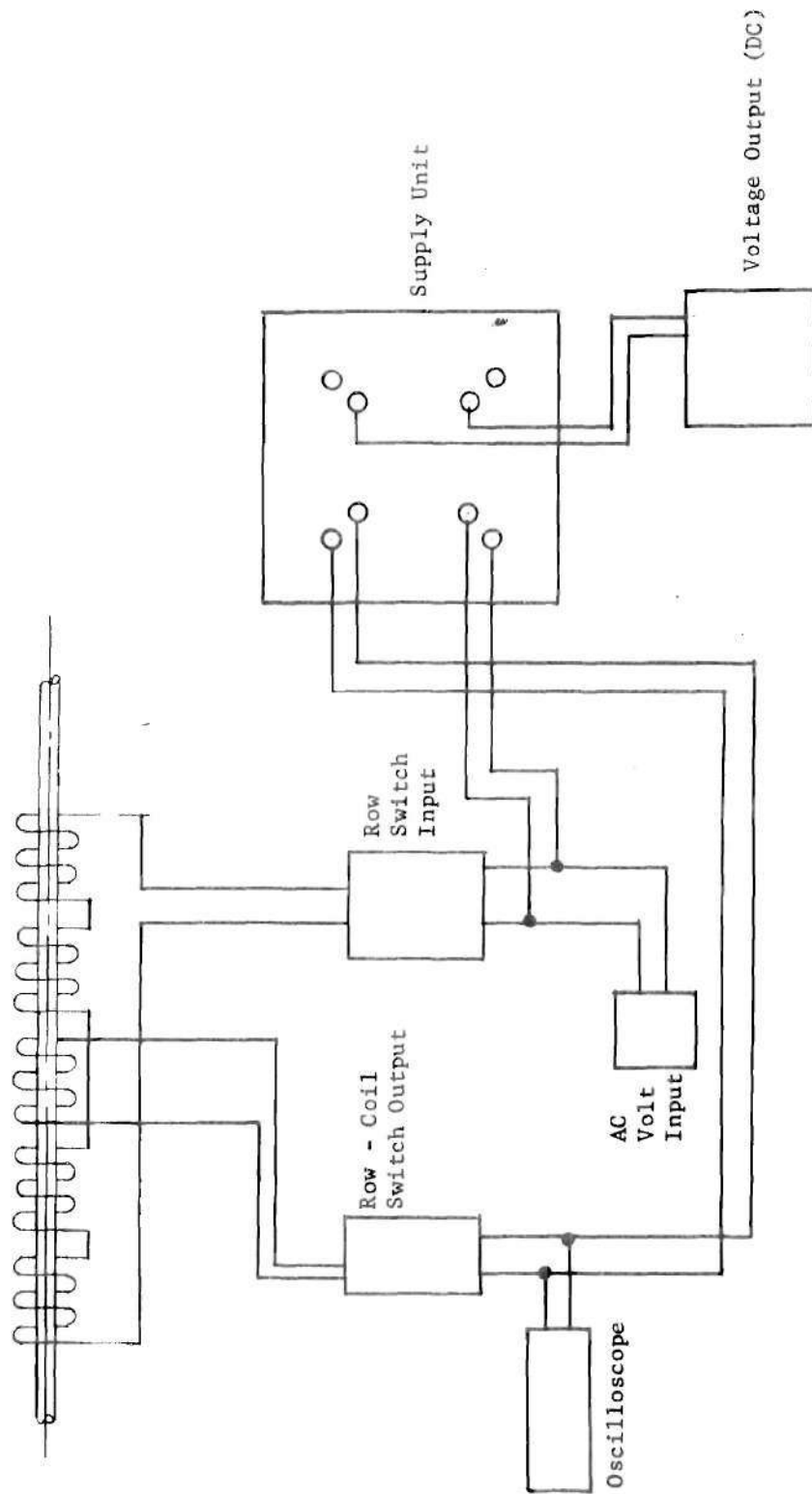


Figure 3. Typical Coil Connection.

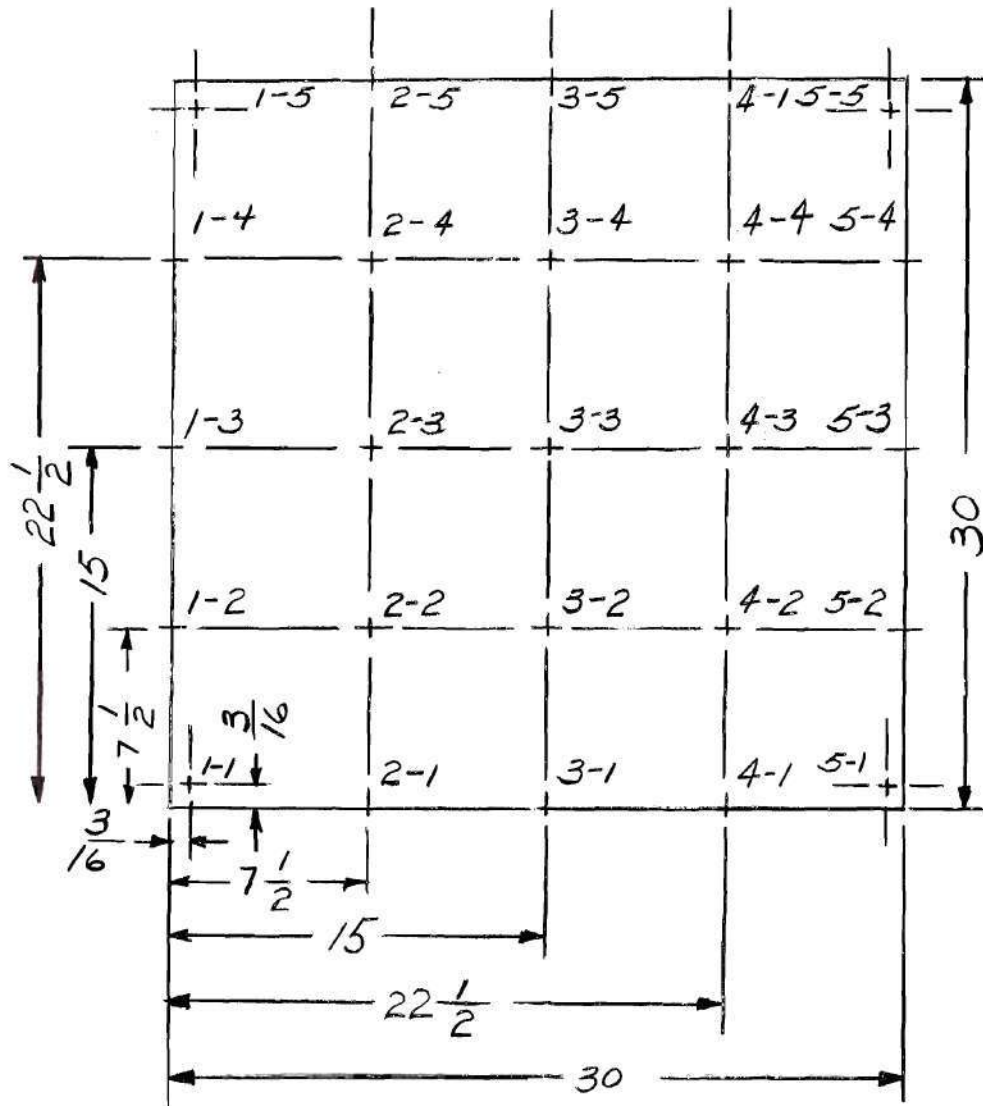


Figure 4. Location of Data Points.

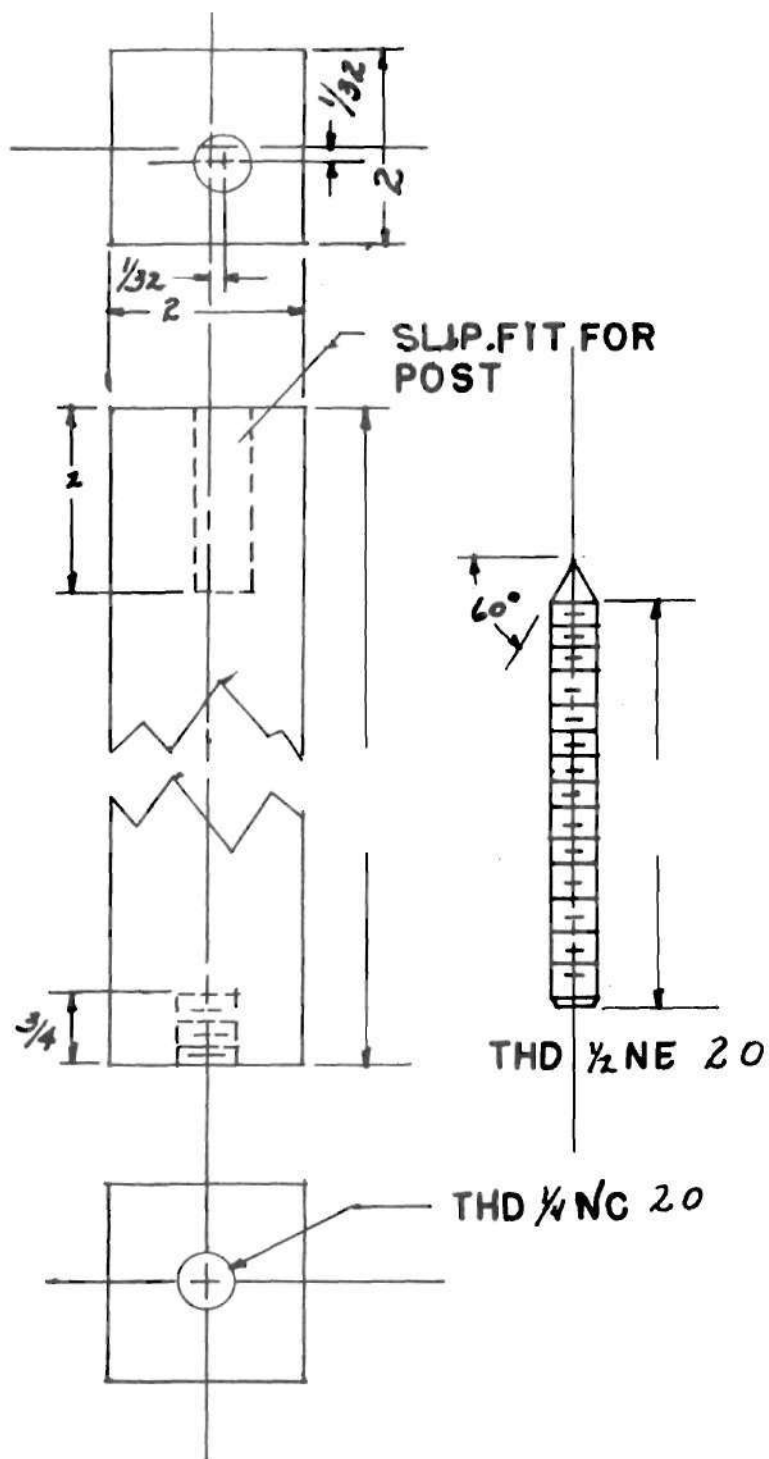
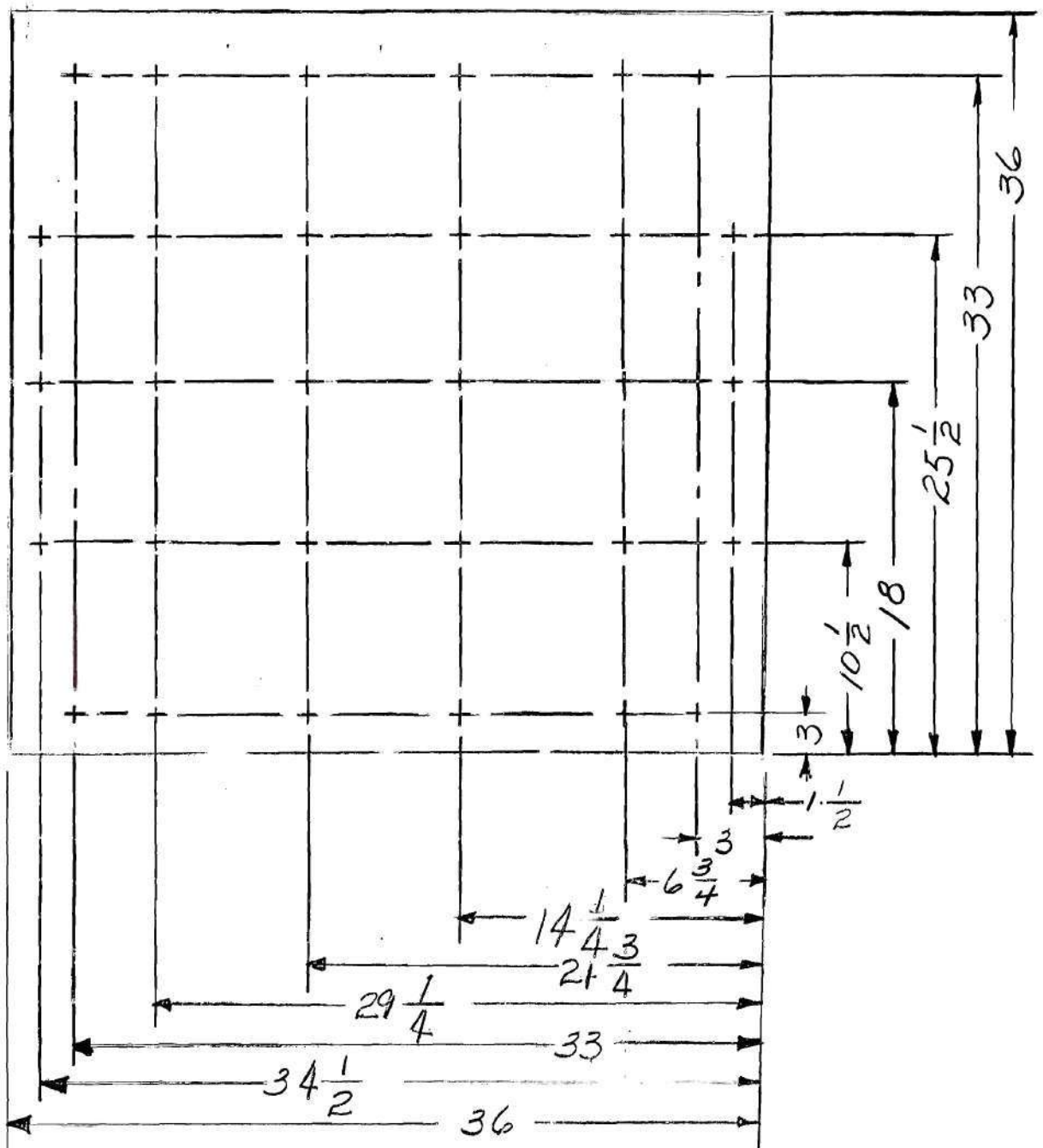


Figure 5. Corner Post Detail.



DR. AND TAP $\frac{1}{4}$ -20

Figure 6. Reference Plate.

Strain gages were attached to the surface of the plate as shown in Figs. 7a and 7b. Interior gages were Baldwin-Lima-Hamilton type FA-25-12-S13 while the gages located along the edge of the plate were Dentronics Type 204C-13. Baldwin-Lima-Hamilton EPY 150 cement was chosen as the bonding media because it appeared to have one of the highest strain limits for a room curing commercial epoxy cement. After sufficient time for curing had been allowed the gages were wired as shown in Fig. 6.

The control panel, Fig. 8, shows the relative location of all the input-output equipment used in the performance of this experiment.

Test Procedures

Two methods of achieving various load configurations on the plate were attempted. Initially, sand was distributed in the frame shown in Fig. 9 to represent the various loading conditions. However, variation in distribution of the sand resulted in variations in deflection and strain readings for repeated loads and thus made repeatability almost impossible. However, concentrated weights symmetrically placed to simulate various loading conditions produced experimental measurements which could be repeated with little or no deviation. Although it was recognized that concentrated weights did induce actual discontinuities in the load supported by the plate this error was felt to be negligible.

Strain and deflection measurements were made independently of one another. The plate was placed so as to allow the strain gages to be entirely free of the pressure of the small concentrated weights. Present strain gage literature seems to indicate extremely large hydrostatic pressures must be used to significantly influence variations in strains due to lateral loading. However, this secondary effect, often neglected, seriously influences the values of small strain measurements.



Figure 7a. Strain Gage Placement on the Plate Surface.



Figure 7b. Strain Gage Placement on the Plate Surface.

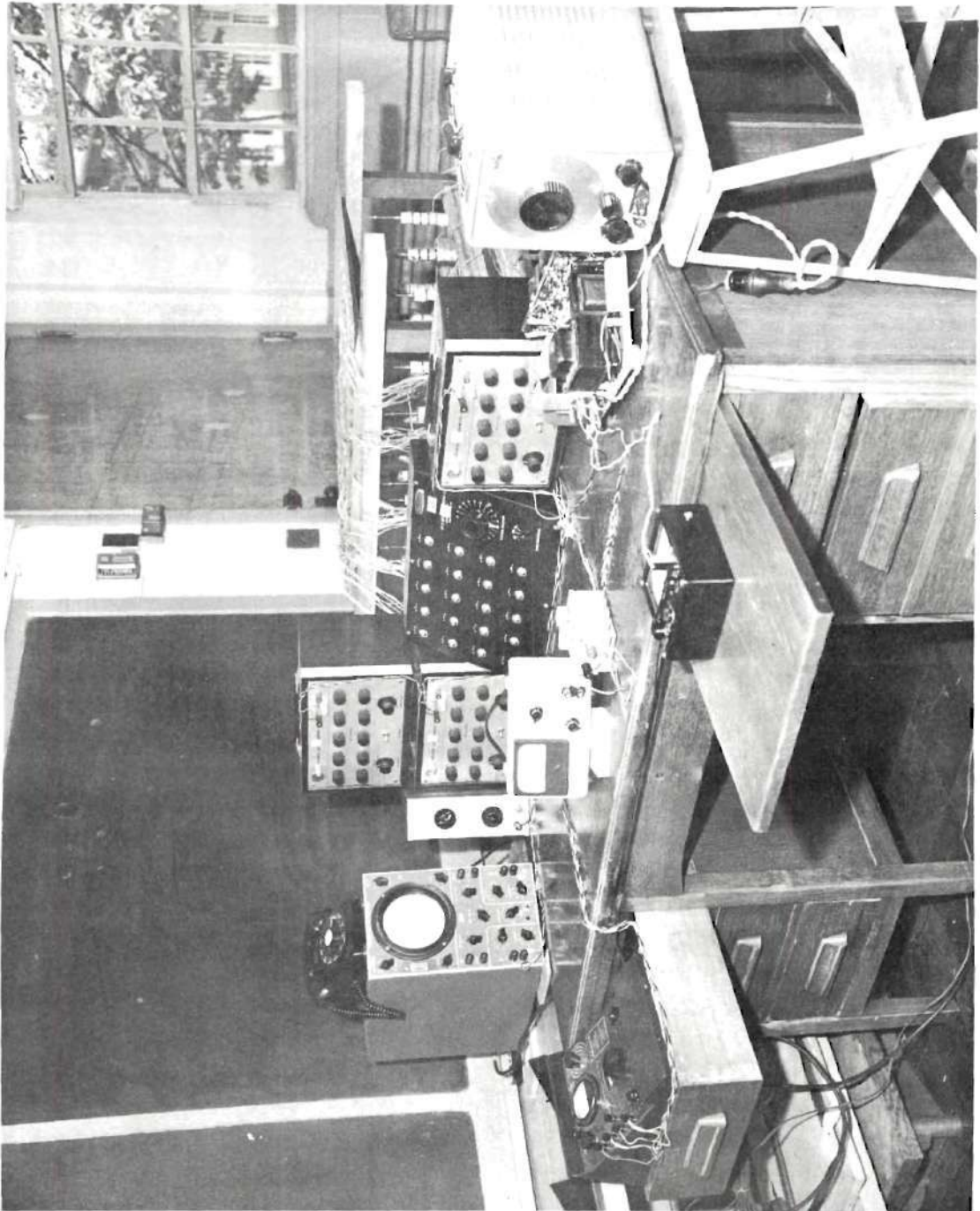


Figure 8. Control Panel.

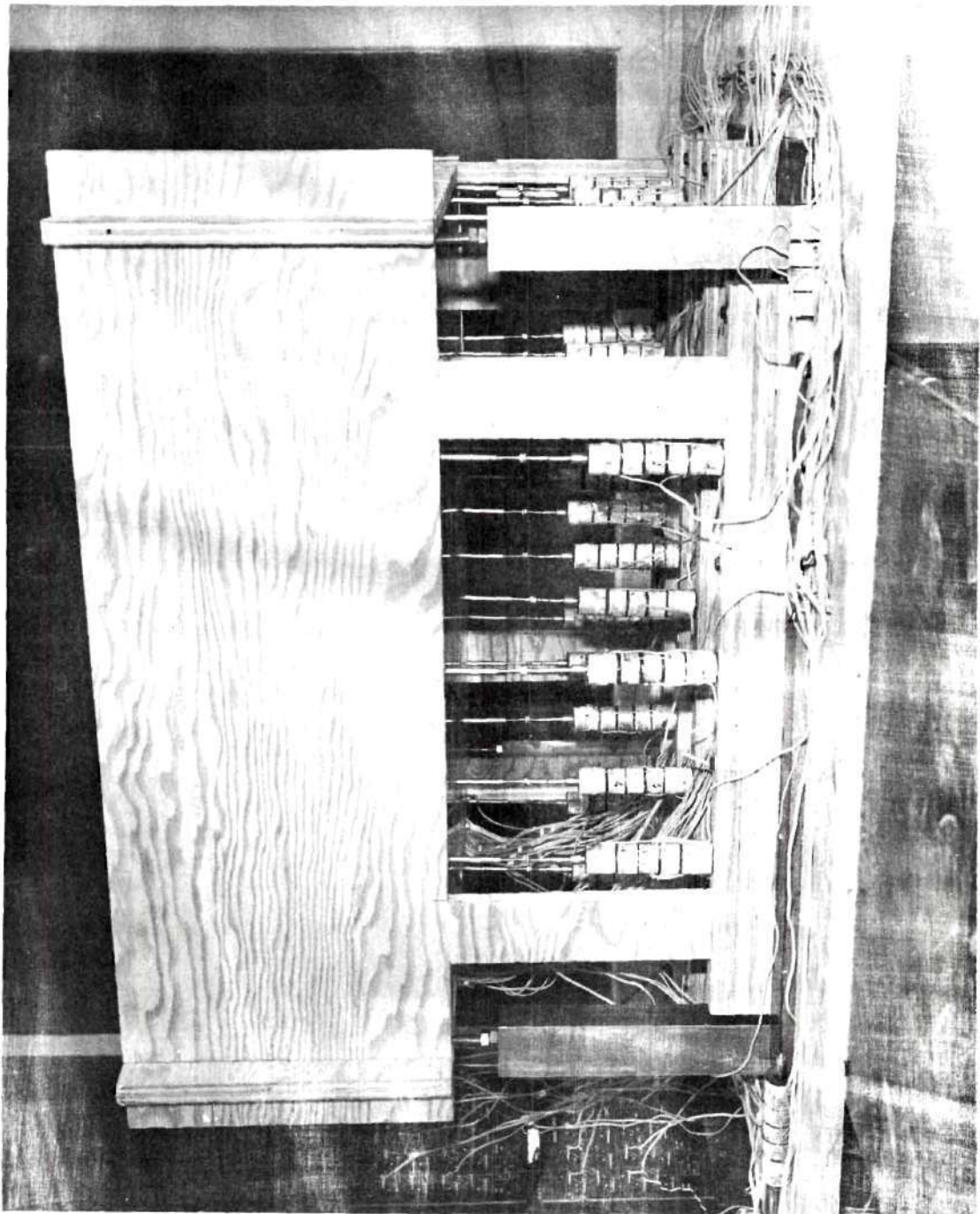


Figure 9. Loading Frame.

An easy way to convince oneself of the existence of this error is to perform a standard bond integrity test by lightly pressing a pencil eraser into a strain gage. If a good bond exists then the gage will indicate a slight strain and return to zero when the load is removed.

After completion of the strain measurements the plate was similarly loaded and deflection measurements were made using the differential transformers previously described.

Data Analysis

Conversion of the strain data obtained from the strain gages to principal stresses was accomplished through the equations describing Hooke's law. Thus the principal stresses and the angle of gage rotation from the principal direction are:

$$\sigma_1 = (T.E.) \left[\frac{\epsilon_a + \epsilon_b + \epsilon_c}{3(1-\nu)} + \frac{1}{1+\nu} \sqrt{\left(\epsilon_a - \frac{\epsilon_a + \epsilon_b + \epsilon_c}{3} \right)^2 + \left(\frac{\epsilon_c - \epsilon_b}{3} \right)^2} \right] \quad (88)$$

$$\sigma_2 = (T.E.) \left[\frac{\epsilon_a + \epsilon_b + \epsilon_c}{3(1-\nu)} - \frac{1}{1+\nu} \sqrt{\left(\epsilon_a - \frac{\epsilon_a + \epsilon_b + \epsilon_c}{3} \right)^2 + \left(\frac{\epsilon_c - \epsilon_b}{3} \right)^2} \right] \quad (89)$$

$$\tau_{MAX} = 2GT \sqrt{\left(\frac{\epsilon_a - \epsilon_b + \epsilon_b + \epsilon_c}{3} \right)^2 + \left(\frac{\epsilon_c - \epsilon_b}{3} \right)^2} \quad (90)$$

$$\phi = \frac{1}{2} \text{TAN}^{-1} \left[\frac{\sqrt{3} \epsilon_c - \epsilon_b}{2 \epsilon_c - \epsilon_b - \epsilon_c} \right] \quad (91)$$

These equations were used in the computer program on page 96 to calculate the principal stresses on pages 55 to 78.

Determination of the output voltage readings of the differential transformers required a conversion factor when switching scales. The following equations were derived to accomplish this purpose.

$$V_T = V_R \quad 0 \leq RV \leq 2.5 \quad (92)$$

$$V_T = 0.813521 V_R + 0.00124 \quad 2.5 \leq RV \leq 10 \quad (93)$$

$$V_T = 0.813521 (V_R - 0.50) + 0.00124 \quad 10 \leq RV \leq 50 \quad (94)$$

The accuracy of the output voltage does not warrant equations involving six decimal place accuracy; however, it was felt that the overall round-off error would be less if this accuracy was used.

Conversion of the D-C voltage output of each coil to deflections was achieved with a micrometer screw, containing 40 threads per inch as shown in Fig. 10. Output voltages, corrected by equations (92), (93) and (94), were recorded at intervals of 0.025 inches for each coil. Averaging a series of three readings for each coil and applying the method of least squares to an equation of a straight line, one obtains the following 24 calibration equations for the given locations.

<u>Location</u>	<u>Equation</u>	
1-1	$W = (0.0207344)V_T - (0.00273738)$	(95)

1-2	$W = (0.02160861)V_T - (0.002790185)$	(96)
-----	---------------------------------------	------

1-3	$W = (0.02175900)V_T - (0.003160176)$	(97)
-----	---------------------------------------	------

1-4	$W = (0.02218708)V_T - (0.002231466)$	(98)
-----	---------------------------------------	------

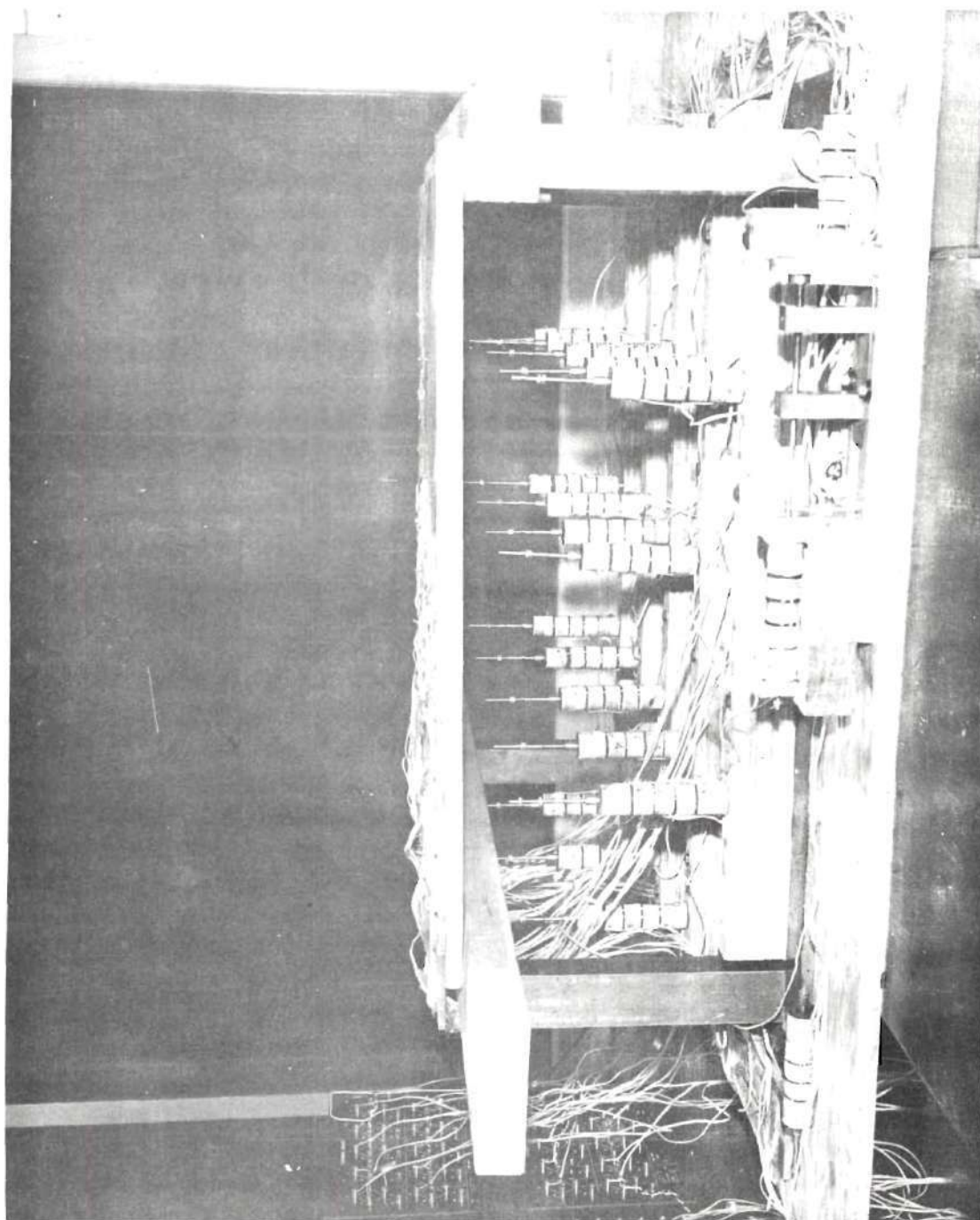


Figure 10. Coil Calibration.

<u>Location</u>	<u>Equation</u>	
1-5	$W = (0.02198784)V_T - (0.001434582)$	(99)
2-1	$W = (0.02159086)V_T - (0.002676522)$	(100)
2-2	$W = (0.02928728)V_T - (0.003800911)$	(101)
2-3	$W = (0.02501338)V_T - (0.004559467)$	(102)
2-4	$W = (0.02130784)V_T - (0.00275113)$	(103)
2-5	$W = (0.02202942)V_T - (0.00317116)$	(104)
3-1	$W = (0.0225732)V_T - (0.003259863)$	(105)
3-2	$W = (0.02041016)V_T - (0.002049275)$	(106)
3-3	$W = (0.01904081)V_T - (0.001360606)$	(107)
3-4	$W = (0.05066258)V_T - (0.007381442)$	(108)
3-5	$W = (0.02131003)V_T - (0.00366149)$	(109)
4-1	$W = (0.02144298)V_T - (0.003023097)$	(110)
4-2	$W = (0.01939309)V_T - (0.002050768)$	(111)
4-3	$W = (0.012949647)V_T - (0.0026578381)$	(112)
4-4	$W = (0.02268241)V_T - (0.003209228)$	(113)
4-5	$W = (0.02257066)V_T - (0.004050783)$	(114)
5-1	$W = (0.02124027)V_T - (0.002354510)$	(115)

<u>Location</u>	<u>Equation</u>	
5-2	$W = (0.02134929)V_T - (0.003259926)$	(116)

5-3	$W = (0.02283902)V_T - (0.005008836)$	(117)
-----	---------------------------------------	-------

5-4	$W = (0.02170540)V_T - (0.003390082)$	(118)
-----	---------------------------------------	-------

Equations (92) through (94) and (95) through (118) were applied to the D-C output voltage through the computer program on page to determine the deflection data for various representative loads presented on pages 55 to 78.

CHAPTER IV

RESULTS

Maximum principal stresses and deflections at points on the interior and on the boundary of a plate supported at four corners have been obtained by analytical and experimental techniques. The data for both methods is presented on pages 55 to 88. The results of the experimental analysis contain measurements for symmetrical and non-symmetrical loadings while the analytical data contains only valid values for a uniform load. No attempt has been made to compare the maximum principal stresses and deflections due to unsymmetrical loadings to theoretical predictions. These data have been presented for future reference and completeness.

Linear plate theory was assumed throughout the analytical investigation. The validity of this assumption is evident in the stress and deflection data for the symmetrical and non-symmetrical loadings. An increase in load shows a proportional increase in the deflections. This confirms the premise "Linear plate theory is applicable if the deflections are less than half the thickness of the plate."

Inspection suggests various points in a rectangular plate with symmetrical loadings should have common values of deflection and maximum principal stress. Application of this reasoning to a square plate suggests identities exist in the following sets of locations. (Refer to Fig. 4 page 29 for geometric location).

<u>Set I</u>	<u>Set II</u>	<u>Set III</u>	<u>Set IV</u>
1-2 4-1	1-3	2-2	2-3
1-4 4-5	3-1	2-4	3-2
2-1 5-2	3-5	4-2	3-4
2-5 5-4	5-3	4-4	4-3

The deflections and maximum principal stresses at each set of locations for a 42 lb. total uniform load are recorded in the following tables.

Table 1. Set I

Location	<u>Stress psi</u>		Deflection in.
	Max.	Min.	
1-2	402		.032
1-4			.033
2-1	411		.024
2-5			.025
4-1	325		.026
4-5			.026
5-2	421		.032
5-4			.034

Table 2. Set II

Location	<u>Stress psi</u>		Deflection in.
	Max.	Min.	
1-3	564		.047
3-1	450		.036
3-5			.037
5-3	564		.048

Table 3. Set III

Location	Stress psi		Deflection in.
	Max.	Min.	
2-2	411		.064
2-4			.044
4-2	379		.042
4-4			.048

Table 4. Set IV

Location	Stress psi		Deflection in.
	Max.	Min.	
2-3	453		.054
3-2	446		.047
3-4			.120
4-3	457		.030

The experimental data in the above tables, and on pages 55 to 78 of the appendix show the deflections predicted by the instruments located at 2-2, 3-4, and 4-3 are inconsistent with readings at other symmetrically located geometric points. Thus, these three instruments indicated data of questionable value.

The reliability and reproducibility of the electrical systems used in the experimental investigation were excellent. To obtain the measurements on pages 55 to 78 a series of three readings were made. In all instances the differences in similar geometric points were caused by systematic error. This reproducibility showed that the system used to determine deflection and stress had errors of less than five per cent.

The polynomial and trigonometric shape functions involving two parameters, excluding A_{00} , with uniformly distributed loads predicted deflections and stresses which are in agreement with the experimental values. The deflection predicted by the trigonometric series is within 0.001 in. of the experimental value at the center of the plate but disagreed slightly at various other locations on the plate due primarily to the lack of isotropicity of the material. The stresses predicted by this function are higher than the experimental values, thus indicating that the function is on the "safe side" in engineering analysis.

The stresses and deflections predicted by the two parameter polynomials are somewhat less than those predicted by the trigonometric expression. Agreement between the experimental and analytical values of deflection for this function is not as good as in the previous case. However, agreement in stresses is quite close.

The deflection and stresses predicted by the three parameter trigonometric and polynomial shape function of page 12 and 18 closely approximate the experimental results on page 64 . The deflections predicted by the three parameter trigonometric function are greater than the experimental results. However, the stresses are less. Also, differences exist between this solution and the assumed two parameter solutions. These differences are the result of the additional third parameter which can improve the solution at one point while causing larger errors to exist at other points. This discrepancy could be resolved by taking a larger number of terms. If a more accurate solution is necessary, it cannot be achieved through the simple addition of one parameter but must be accomplished by adding all combinations of additional terms of equal relative importance. Comparison of the maximum theoretical deflections, predicted the shape function on page 18 , and the measured deflections showed agreement to be .004 or .008 in. better than the maximum deflection predicted by the shape function of page 20 .

CHAPTER V

CONCLUSIONS

1. Comparison of the experimental and analytical results for symmetrical loads showed:

a. The stresses and deflections predicted by shape functions satisfying the geometrical boundary conditions approximated the measured values. Closest agreement between experimental and theoretical deflections occurred with the two parameter trigonometric shape functions; but, the stresses were best approximated by the three parameter polynomial shape function. However, agreement with experimental data was sufficiently good to indicate the validity of all of the shape functions used.

b. Classical plate theory gives useful information about stresses and deflections for non-developable surfaces, if the deflections are of the same order of magnitude as the thickness of the plate.

2. Analysis of the experimental systems used in this investigation showed:

a. The differential transformers proved to be a reliable method of measuring plate deflections. Under similar loading conditions, the magnitudes of the readings were repeatable within one percent. The sensitivity of the differential transformers was sufficient to record as little as one percent variation in the load.

b. Measurements of small strains can be made with strain gages. These values are repeatable within five per cent error provided

no lateral pressure is applied to the strain gages.

3. Comparison of the various deflection equations obtained through theoretical analysis, evaluated for a square plate supporting a uniform load, favorably agree with solutions presented by Timoshenko.

Recommendations

Analytical investigation of rectangular plates supported at four corners has presently been limited to plates supporting symmetric loads. Non-symmetrical loading conditions are often encountered in reality and it is recommended that further analytical works needs to be done in this area.

A literature survey which was initially undertaken to ascertain the amount of previous work done on discontinuously supported rectangular plates yielded little information. This search carried the author into mechanical engineering, engineering mechanics, civil engineering and mathematical engineering journals and various other sources. Through this it was recognized that little work had been done on rectangular plates with discontinuous boundary supports. Presently, plans are being made to further investigate plates with both symmetric and non-symmetric loads.

APPENDIX

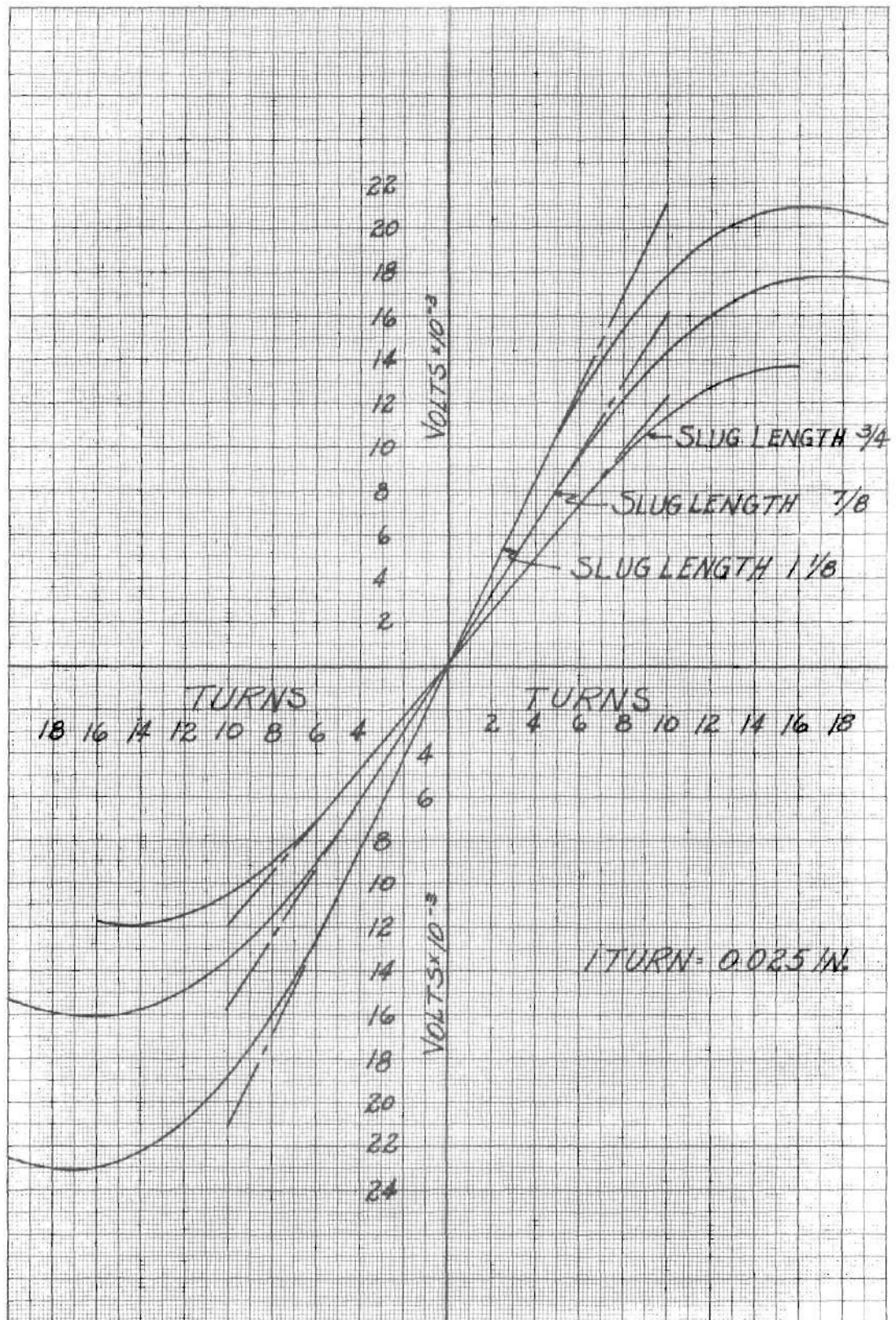


Figure 11a. Evaluation of a Configuration for Five Small Coils.

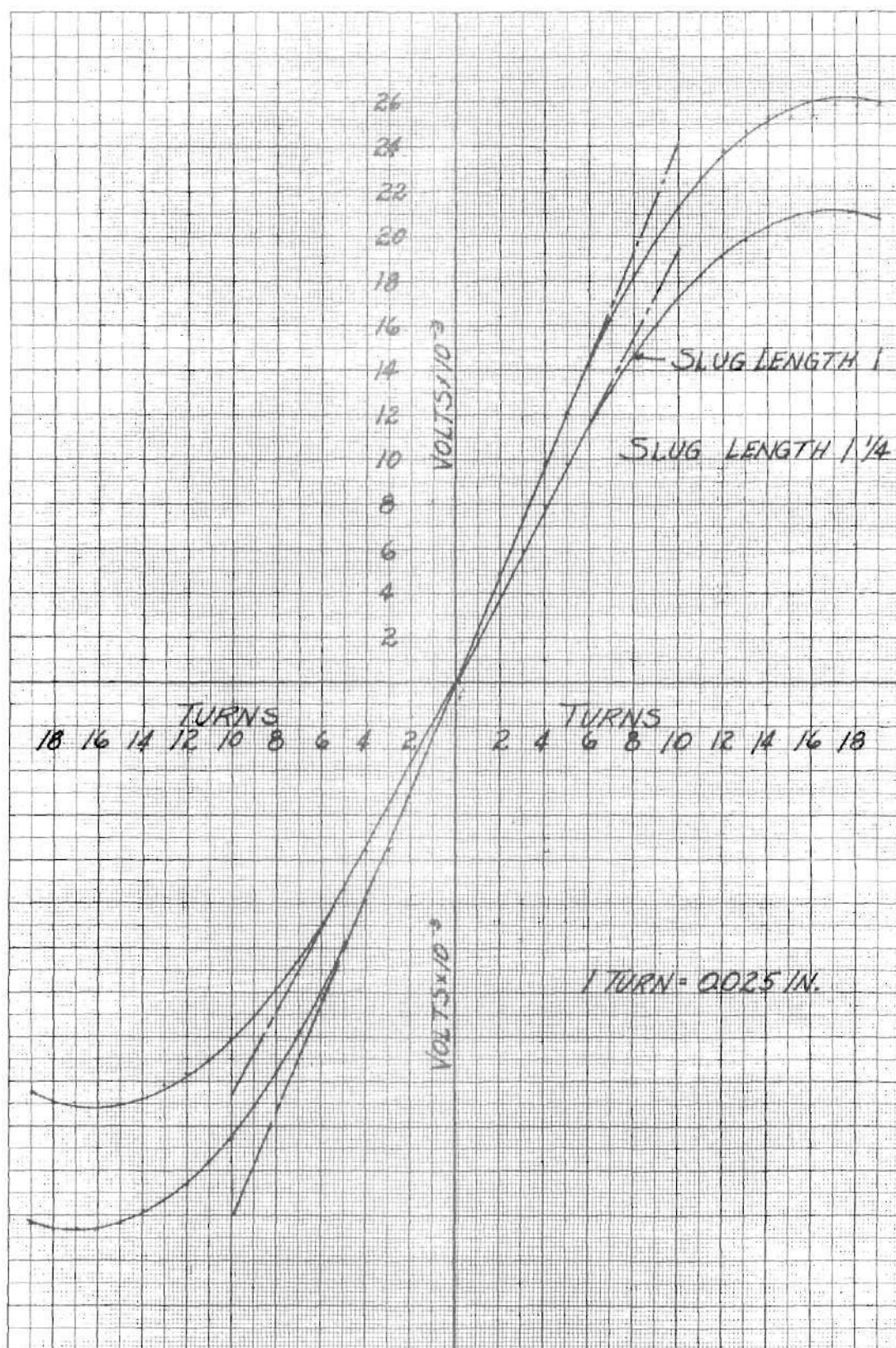


Figure 11b. Evaluation of a Configuration for Five Small Coils.

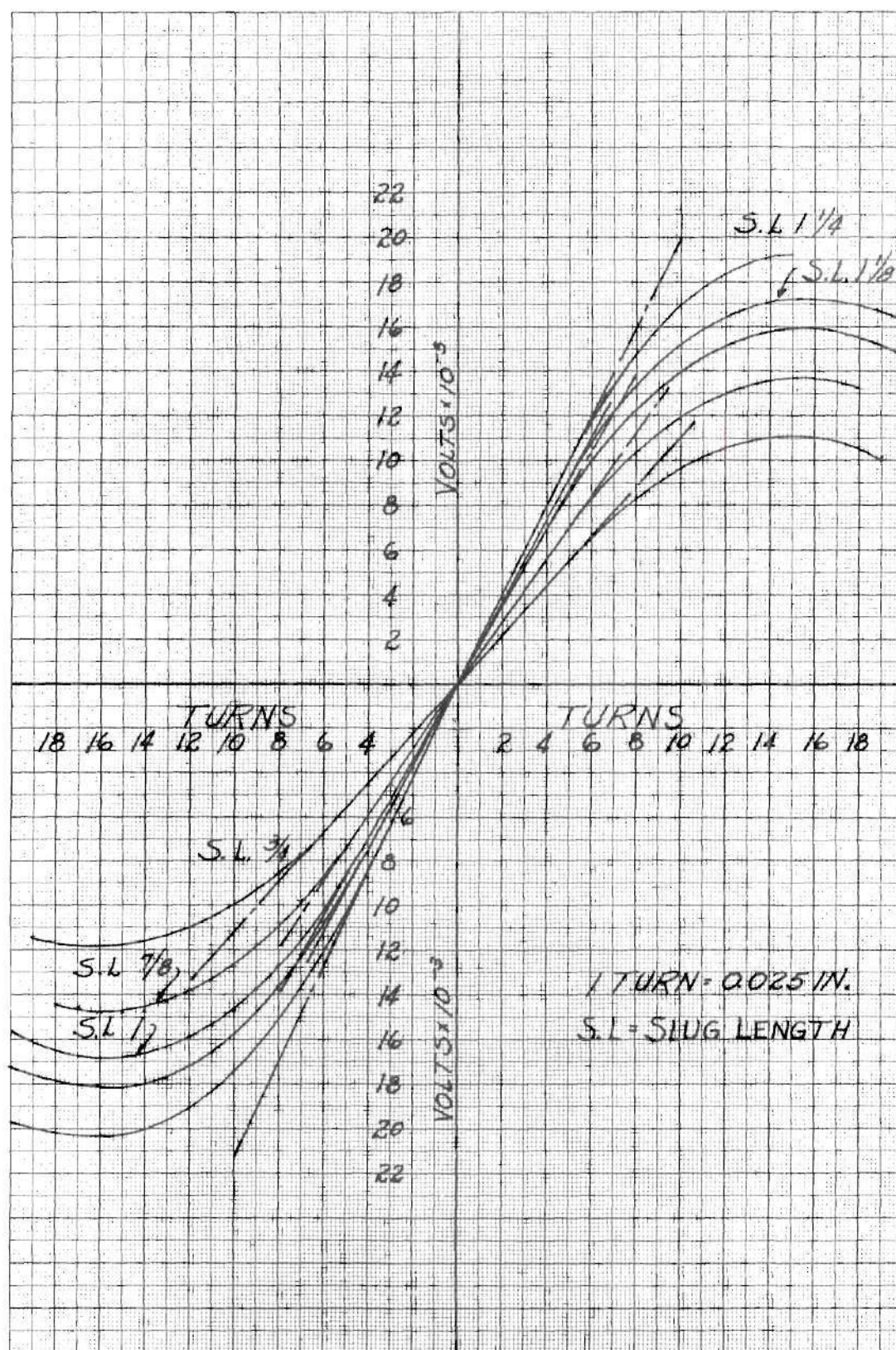


Figure 12. Evaluation of a Configuration for Three Small Coils.

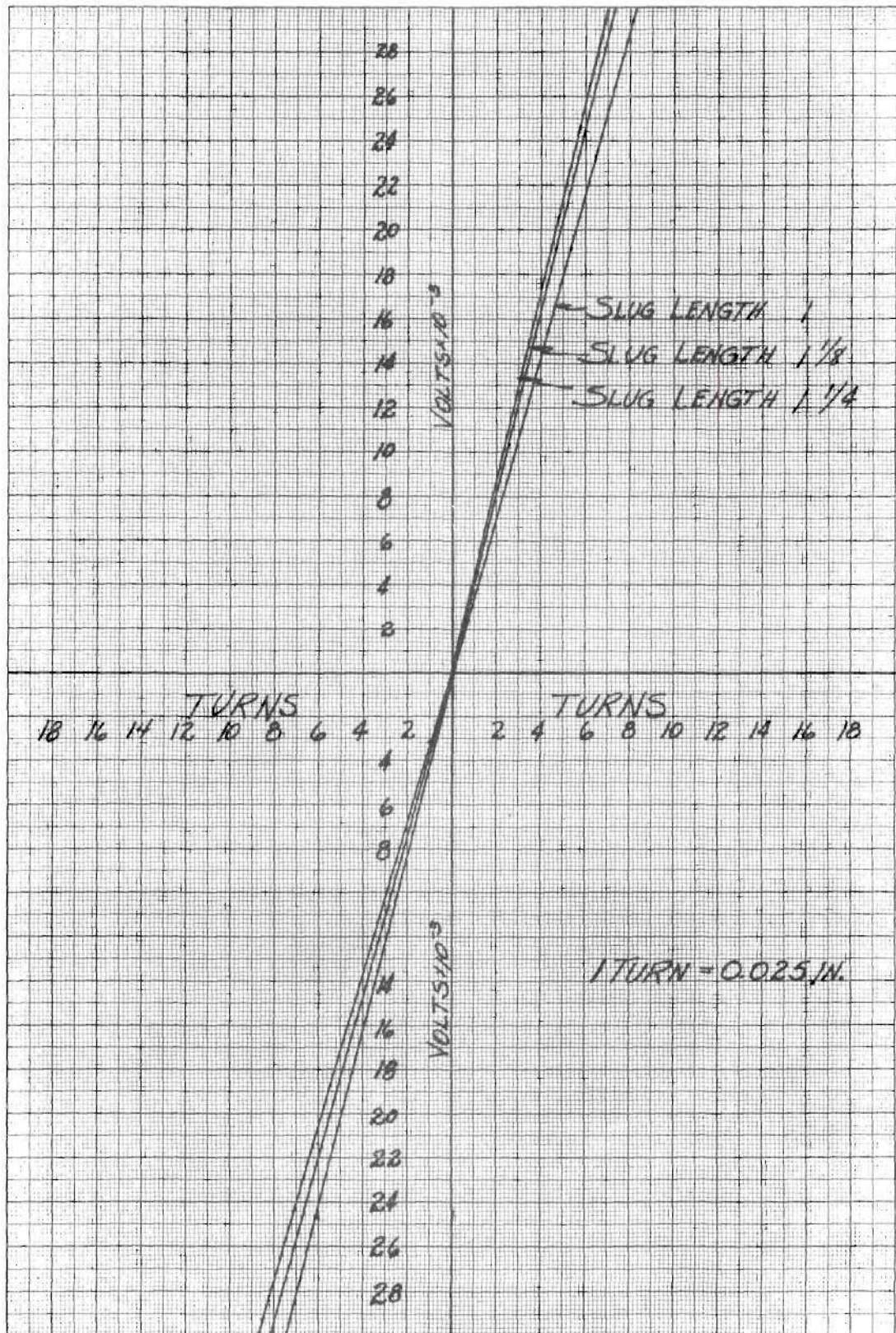


Figure 13a. Evaluation of a Configuration for Two Large Coils Symmetric with Three Small Coils.

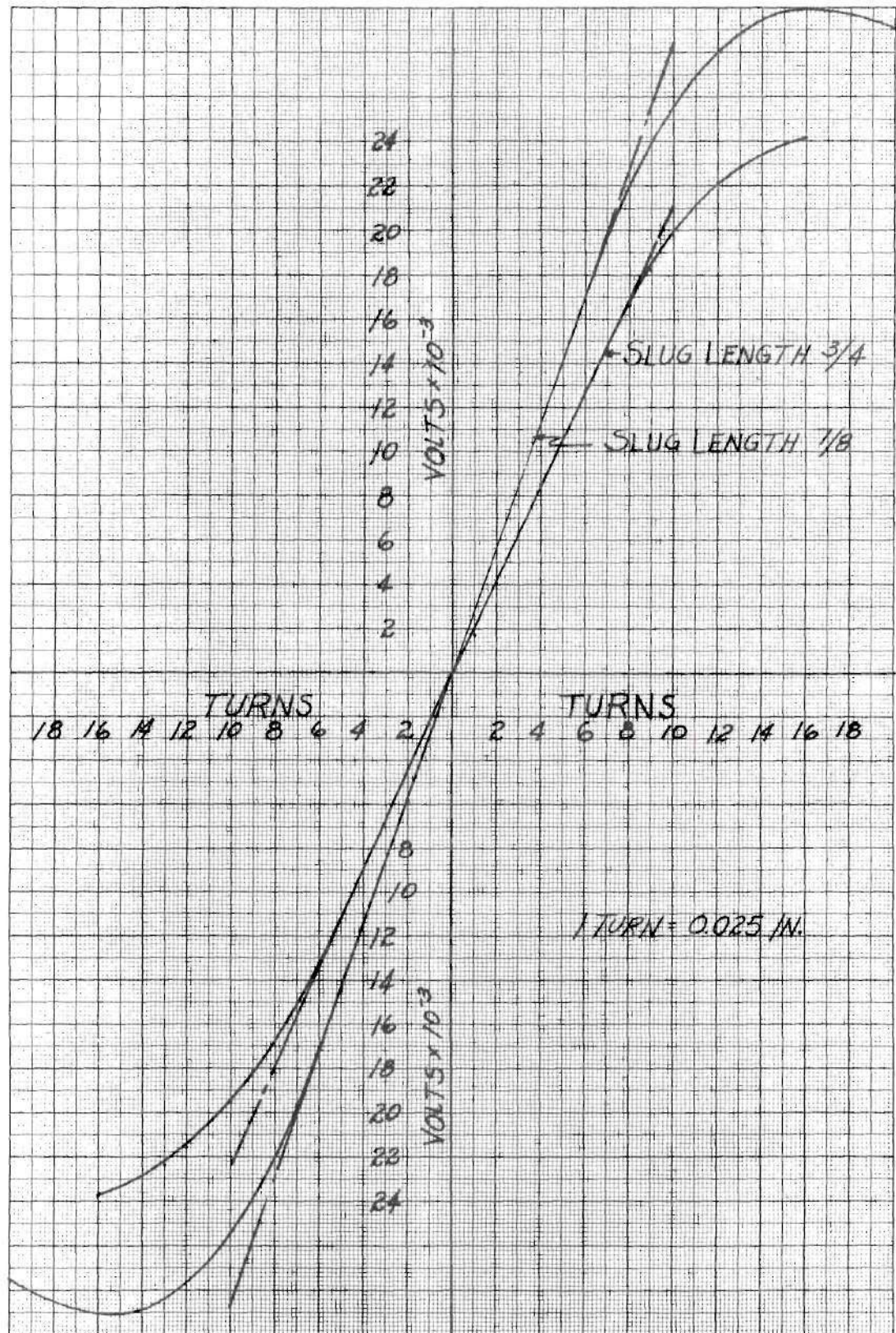


Figure 13b. Evaluation of a Configuration for Two Large Coils Symmetric with Three Small Coils.

Table 5. Experimental Data

Type of Load Concentrated on DiagonalsWeight of Load 34

Location	Deflection in.	σ Max. Psi	σ Min. Psi
1-1			
1-2	.028	459	
1-3	.037	230	
1-4	.023		
1-5			
2-1	.026	373	
2-2	.063	337	129
2-3	.048	380	277
2-4	.037		
2-5	.022		
3-1	.034	459	
3-2	.037	395	291
3-3	.047	437	296
3-4	.116		
3-5	.034		
4-1	.023	488	
4-2	.035	597	412
4-3	.025	377	299
4-4	.047		
4-5	.027		
5-1			
5-2	.023	478	
5-3	.037	493	
5-4	.029		
5-5			

Table 18. Experimental Data

Type of Load Concentrated on DiagonalsWeight of Load 54

Location	Deflection in.	σ Max. Psi	σ Min. Psi
1-1			
1-2	.046	383	
1-3	.062	708	
1-4	.038		
1-5			
2-1	.043	421	
2-2	.103	536	245
2-3	.077	605	442
2-4	.060		
2-5	.036		
3-1	.056	593	
3-2	.072	642	482
3-3	.078	721	488
3-4	.179		
3-5	.055		
4-1	.036	766	
4-2	.059	962	638
4-3	.042	611	494
4-4	.076		
4-5	.043		
5-1			
5-2	.038	756	
5-3	.060	679	
5-4	.046		
5-5			

Table 7. Experimental Data

Type of Load Concentrated on Diagonals
 Weight of Load 72

Location	Deflection	σ Max.	σ Min.
1-1			
1-2	.082	947	
1-3	.121	1828	
1-4	.082		
1-5			
2-1	.044	660	
2-2	.149	902	441
2-3	.128	1490	653
2-4	.100		
2-5	.044		
3-1	.063	785	
3-2	.104	751	25
3-3	.125	1421	845
3-4	.262		
3-5	.064		
4-1	.045	641	
4-2	.095	405	252
4-3	.068	664	417
4-4	.111		
4-5	.042		
5-1			
5-2	.084	967	
5-3	.117	1751	
5-4	.081		
5-5			

Table 7. Experimental Data

Type of Load Center Load on 16 in² Area
 Weight of Load 32

Location	Deflection in.	σ Max. Psi	σ Min. Psi
1-1			
1-2	.029	373	
1-3	.044	574	
1-4	.031		
1-5			
2-1	.027	392	
2-2	.071	427	325
2-3	.060	601	380
2-4	.048		
2-5	.029		
3-1	.040	555	
3-2	.055	601	399
3-3	.063	822	806
3-4	.139		
3-5	.040		
4-1	.027	392	
4-2	.045	406	299
4-3	.031	588	355
4-4	.052		
4-5	.027		
5-1			
5-2	.029	383	
5-3	.040	555	
5-4	.028		
5-5			

Table 8. Experimental Data

Type of Load Center Load on 16 in² Area
 Weight of Load 48

Location	Deflection in.	σ Max. Psi	σ Min. Psi
1-1			
1-2	.045	545	
1-3	.065	804	
1-4	.045		
1-5			
2-1	.042	574	
2-2	.108	617	468
2-3	.089	887	560
2-4	.072		
2-5	.043		
3-1	.061	775	
3-2	.083	872	575
3-3	.097	1157	1147
3-4	.211		
3-5	.062		
4-1	.042	565	
4-2	.069	509	
4-3	.048	845	812
4-5	.042		
5-1			
5-2	.045	574	
5-3	.063	775	
5-4	.043		
5-5			

Table 9. Experimental Data

Location	Type of Load	Center Load on 16 in ² Area	
	Weight of Load	64	
Location	Deflection in.	σ Max. Psi	σ Min. Psi
1-1			
1-2	.059	708	
1-3	.087	1062	
1-4	.060		
1-5			
2-1	.055	756	
2-2	.142	839	580
2-3	.118	1166	748
2-4	.096		
2-5	.057		
3-1	.081	1024	
3-2	.110	1173	760
3-3	.129	1547	1528
3-4	.211		
3-5	.082		
4-1	.056	727	
4-2	.092	822	530
4-3	.063	1130	698
4-4	.107		
4-5	.056		
5-1			
5-2	.060	766	
5-3	.082	1033	
5-4	.063		
5-5			

Table 10. Experimental Data

Location	Deflection in.	Type of load	Edge
		Weight of Load	80
1-1			
1-2	.047		612
1-3	.067		746
1-4	.048		
1-5			
2-1	.045		651
2-2	.097		560
2-3	.077		494
2-4	.065		
2-5	.046		
3-1	.064		737
3-2	.071		515
3-3	.075		395
3-4	.179		
3-5	.063		
4-1	.046		756
4-2	.064		561
4-3	.041		480
4-4	.071		
4-5	.045		
5-1			
5-2	.046		699
5-3	.065		737
5-4	.045		
5-5			

Table 11. Experimental Data

Location	Type of Load	Edge	
	Weight of Load	48	
Location	Deflection in.	σ Max. Psi	σ Min. Psi
1-1			
1-2	.027	373	
1-3	.039	450	
1-4	.028		
1-5			
2-1	.026	402	
2-2	.056	321	79
2-3	.045	265	135
2-4	.038		
2-5	.027		
3-1	.036	440	
3-2	.041	294	172
3-3	.044	228	228
3-4	.104		
3-5	.036		
4-1	.026	440	
4-2	.035	334	85
4-3	.023	272	147
4-4	.041		
4-5	.027		
5-1			
5-2	.026	421	
5-3	.036	440	
5-4	.026		
5-5			

Table 12. Experimental Data

Type of Load VEEWeight of Load 105

Location	Deflection in.	σ Max. Psi	σ Min. Psi
1-1			
1-2	.084	1167	
1-3	.118	1445	
1-4	.084		
1-5			
2-1	.060	880	
2-2	.158	932	382
2-3	.128	1088	540
2-4	.104		
2-5	.059		
3-1	.085	861	
3-2	.112	709	700
3-3	.125	948	604
3-4	.277		
3-5	.080		
4-1	.061	919	
4-2	.102	940	345
4-3	.068	1068	599
4-5	.052		
5-1			
5-2	.081	1196	
5-3	.112	1426	
5-4	.082		
5-5			

Table 13. Experimental Data

Type of Load Pyramid
 Weight of Load 83

Location	Deflection in.	σ Max. Psi	σ Min. Psi
1-1			
1-2	.047	880	
1-3	.069	1158	
1-4	.048		
1-5			
2-1	.046	861	
2-2	.108	979	563
2-3	.088	1144	770
2-4	.073		
2-5	.046		
3-1	.066	1072	
3-2	.082	1115	846
3-3	.090	1235	1184
3-4	.206		
3-5	.066		
4-1	.047	842	
4-2	.068	967	518
4-3	.046	1102	879
4-4	.079		
4-5	.045		
5-1			
5-2	.044	890	
5-3	.063	1139	
5-4	.044		
5-5			

Table 14. Experimental Data

Type of Load UniformWeight of Load 42

Location	Deflection in.	σ Max. Psi	σ Min. Psi
1-1			
1-2	.032	402	
1-3	.047	564	
1-4	.033		
1-5			
2-1	.024	344	
2-2	.064	411	208
2-3	.054	453	261
2-4	.044		
2-5	.025		
3-1	.036	450	
3-2	.047	372	314
3-3	.052	446	335
3-4	.120		
3-5	.037		
4-1	.026	325	
4-2	.042	379	135
4-3	.030	459	255
4-4	.048		
4-5	.026		
5-1			
5-2	.032	421	
5-3	.048	564	
5-4	.034		
5-5			

Table 15. Experimental Data

Type of Load Uniform
 Weight of Load 63

Location	Deflection in.	σ Max. Psi	σ Min. Psi
1-1			
1-2	.048	660	
1-3	.069	842	
1-4	.048		
1-5			
2-1	.035	478	
2-2	.093	611	293
2-3	.077	681	385
2-4	.063		
2-5	.036		
3-1	.051	489	
3-2	.067	586	480
3-3	.075	672	556
3-4	.171		
3-5	.054	469	
4-1	.037		
4-2	.059	584	244
4-3	.040	645	355
4-4	.035		
5-1			
5-2	.046	679	
5-3	.065	823	
5-4	.046		
5-5			

Table 16. Experimental Data

Type of Load Uniform
 Weight of Load 84

Location	Deflection in.	σ Max. Psi	σ Min. Psi
1-1			
1-2	.067	804	
1-3	.095	1139	
1-4	.072		
1-5			
2-1	.058	660	
2-2	.135	816	413
2-3	.108	930	546
2-4	.091		
2-5	.054		
3-1	.077	947	
3-2	.100	799	640
3-3	.111	872	727
3-4	.252		
3-5	.077		
4-1	.055	641	
4-2	.088	803	358
4-3	.061	876	514
4-4	.059		
5-1			
5-2	.066	880	
5-3	.098	1062	
5-4	.068		
5-5			

Table 17. Experimental Data

Type of Load TriangularWeight of Load 75

Location	Deflection in.	σ Max. Psi	σ Min. Psi
1-1			
1-2	.039	507	
1-3	.056	660	
1-4	.040		
1-5			
2-1	.048	622	
2-2	.102	532	306
2-3	.080	615	413
2-4	.068		
2-5	.047		
3-1	.071	842	
3-2	.084	744	503
3-3	.092	689	663
3-4	.212		
3-5	.069		
4-1	.052	832	
4-2	.078	822	272
4-3	.052	618	106
4-4	.090		
4-5	.050		
5-1			
5-2	.062	928	
5-3	.086	1081	
5-4	.064		
5-5			

Table 19. Experimental Data

Type of Load Off Center Load - Position 4-2
 Weight of Load 25

Location	Deflection in.	σ Max. Psi	σ Min. Psi
1-1			
1-2	.037	421	
1-3	.065	785	
1-4	.036		
1-5			
2-1	.017	277	
2-2	.063	435	127
2-3	.057	852	481
2-4	.041		
2-5	.017		
3-1	.026	277	
3-2	.037	355	121
3-3	.043	456	277
3-4	.092		
3-5	.023		
4-1	.016	1722	
4-2	.025	200	66
4-3	.017	288	93
4-4	.029		
4-5	.015		
5-1			
5-2	.012	191	
5-3	.016	268	
5-4	.012		
5-5			

Table 20. Experimental Data

Type of Load Off Center Load - Position 4-2
 Weight of Load 35

Location	Deflection in.	σ Max. Psi	σ Min. Psi
1-1			
1-2	.054	564	
1-3	.079	1120	
1-4	.053		
1-5			
2-1	.026	383	
2-2	.089	600	209
2-3	.079	1223	691
2-4	.059		
2-5	.025		
3-1	.034	392	
3-2	.053	484	201
3-3	.061	628	372
3-4	.131		
3-5	.058		
4-1	.023	210	
4-2	.037	263	155
4-3	.025	395	138
4-4	.042		
4-5	.021		
5-1			
5-2	.018	268	
5-3	.025	364	
5-4	.018		
5-5			

Table 21. Experimental Data

Type of Load Off Center Load - Position 4-2
 Weight of Load 55

Location	Deflection in.	σ Max. Psi	σ Min. Psi
1-1			
1-2	.087	727	
1-3	.127	1435	
1-4	.086		
1-5			
2-1	.042	217	
2-2	.144	774	282
2-3	.127	1516	873
2-4	.096		
2-5	.043		
3-1	.057	526	
3-2	.087	631	273
3-3	.101	836	487
3-4	.216		
3-5	.055		
4-1	.037	287	
4-2	.055	353	189
4-3	.041	504	172
4-4	.069		
4-5	.063		
5-1			
5-2	.032	316	
5-3	.045	469	
5-4	.032		
5-5			

Table 22. Experimental Data

Type of Load Concentrated Load - Position 3-3
 Weight of Load 25

Location	Deflection in.	σ Max. Psi	σ Min. Psi
1-1			
1-2	.022	191	
1-3	.033	450	
1-4	.023		
1-5			
2-1	.023	297	
2-2	.056	301	223
2-3	.045	458	275
2-4	.037		
2-5	.022		
3-1	.032	431	
3-2	.044	458	285
3-3	.050	732	706
3-4	.114		
3-5	.031		
4-1	.023	287	
4-2	.036	301	241
4-3	.030	443	280
4-4	.041		
4-5	.022		
5-1			
5-2	.021	297	
5-3	.031	440	
5-4	.021		
5-5			

Table 23. Experimental Data

Type of Load Concentrated Load - Position 3-3
 Weight of Load 35

Location	Deflection in.	σ Max. Psi	σ Min. Psi
1-1			
1-2	.031	297	
1-3	.045	584	
1-4	.031		
2-1	.030	402	
2-2	.076	438	334
2-3	.064	680	406
2-4	.051		
2-5	.030		
3-1	.044	564	
3-2	.059	669	411
3-3	.069	1050	949
3-4	.154		
3-5	.042		
4-1	.031	392	
4-2	.049	417	316
4-3	.034	645	393
4-4	.056		
4-5	.031		
5-1			
5-2	.030	402	
5-3	.044	547	
5-4	.030		
5-5			

Table 24. Experimental Data

Type of Load Concentrated Load - Position 3-3
 Weight of Load 45

Location	Deflection in.	σ Max. Psi	σ Min. Psi
1-1			
1-2	.042	421	
1-3	.062	756	
1-4	.042		
1-5			
2-1	.039	517	
2-2	.103	543	409
2-3	.086	851	510
2-4	.069		
2-5	.041		
3-1	.059	737	
3-2	.081	858	522
3-3	.093	1362	1218
3-4	.208		
3-5	.058		
4-1	.042	498	
4-2	.066	538	395
4-3	.046	837	505
4-4	.076		
4-5			
5-1			
5-2	.040	526	
5-3	.059	746	
5-4	.040		
5-5			

Table 25. Experimental Data

Type of Load Concentrated Load - Position 3-3
 Weight of Load 55

Location	Deflection in.	σ Max. Psi	σ Min. Psi
1-1			
1-2	.051	545	
1-3	.074	909	
1-4	.054		
1-5			
2-1	.050	651	
2-2	.126	647	495
2-3	.104	1023	615
2-4	.069		
2-5	.051		
3-1	.071	852	
3-2	.099	1008	619
3-3	.114	1653	1499
3-4	.252		
3-5	.071		
4-1	.051	622	
4-2	.081	659	484
4-3	.056	987	603
4-4	.094		
4-5	.052		
5-1			
5-2	.050	651	
5-3	.071	852	
5-4	.050		
5-5			

Table 26. Experimental Data

Type of Load Outer Loaded Edges
 Weight of Load 32

Location	Deflection in.	σ Max. Psi	σ Min. Psi
1-1			
1-2	.026	220	
1-3	.039	469	
1-4	.026		
1-5			
2-1	.026	249	
2-2	.056	220	
2-3	.046	272	99
2-4	.038		
2-5	.030		
3-1	.038	478	
3-2	.043	294	116
3-3	.045	222	197
3-4	.108		
3-5	.039		
4-1	.028	239	
4-2	.036	298	73
4-3	.024	280	120
4-4	.042		
4-5	.026		
5-1			
5-2	.027	258	
5-3	.039	526	
5-4	.028		
5-5			

Table 27. Experimental Data

Type of Load Outer Loaded Edges
 Weight of Load 48

Location	Deflection in.	σ Max. Psi	σ Min. Psi
1-1			
1-2	.039	373	
1-3	.060	794	
1-4	.030		
1-5			
2-1	.038	383	
2-2	.084	461	129
2-3	.069	436	201
2-4	.057		
2-5	.040		
3-1	.056	766	
3-2	.064	451	235
3-3	.067		
3-4	.161		
3-5	.059		
4-1	.038	383	
4-2	.054	443	110
4-3	.036	445	231
4-4	.063		
4-5	.037		
5-1			
5-2	.039	392	
5-3	.057	804	
5-4	.037		
5-5			

Table 28. Experimental Data

Type of Load Outer Loaded Edges
 Weight of Load 64

Location	Deflection in.	σ Max. Psi	σ Min. Psi
1-1			
1-2	.052	488	
1-3	.078	1100	
1-4	.052		
1-5			
2-1	.050	555	
2-2	.111	602	169
2-3	.090	601	296
2-4	.075		
2-5	.060		
3-1	.074	1052	
3-2	.083	665	315
3-3	.088	479	454
3-4	.211		
3-5	.076		
4-1	.051	517	
4-2	.071	632	148
4-3	.047	603	292
4-4	.082		
4-5	.050		
5-1			
5-2	.053	550	
5-3	.075	1072	
5-4	.050		
5-5			

ALR	.026	BER	.026	MY	5.677	MX	.000	X	.0	Y	.0
W	.053	MX	6.246	SY	545.026	SX	545.026				
W	.053	SX	545.026	MY	5.264	MX	.000	X	7.5	Y	.0
W	.045	MX	4.996	QY	-.000	QX	-.000				
W	.053	QX	-.000	SY	505.418	SX	425.000				
W	.045	SX	425.000	QY	-.000	QX	-.000				
W	.045	QX	-.000	MY	4.268	MX	1.977	X	15.0	Y	.0
W	.026	MX	1.977	SY	409.794	SX	135.232				
W	.026	SX	135.232	QY	-.000	QX	-.000				
W	.026	QX	-.000								
ALR	.026	BER	.026	MY	5.677	MX	.000	X	.0	Y	.0
W	.053	MX	6.246	SY	545.026	SX	545.026				
W	.053	SX	545.026	QYN	-.000	QX	-.000				
W	.053	QX	-.000	MY	4.014	MX	4.417	X	7.5	Y	7.5
W	.037	MX	4.417	SY	385.392	SX	385.392				
W	.037	SX	385.392	QY	-.000	QX	-.000				
W	.037	QX	-.000	MY	.000	MX	.000	X	15.0	Y	15.0
W	.000	MX	.000	SY	.000	SX	.000				
W	.000	SX	.000	QY	-.447	QX	-.447				
W	.000	QX	-.447								

Table 29. Two Parameter Trigonometric Shape Function.

ALD	•020	BED	•020	MY	3.494	MX D	•000	X	•0	Y	•0
W	•040	MX	3.494	SY	335.519						
W	•040	SX	335.519	QY	•000						
W	•040	QX	•000	MY	3.494	MX Y	•000	X	7.5	Y	•0
W	•035	MX	3.494	SY	335.519						
W	•035	SX	335.519	QY	•000						
W	•035	QX	•000	MY	3.494	MX Y	•000	X	15.0	Y	•0
W	•020	MX	3.494	SY	335.519						
W	•020	SX	335.519	QY	•000						
W	•020	QX	•000	MY	3.494	MX Y	•000	X	•0	Y	•0
ALD	•020	BED	•020	SY	335.519						
W	•040	MX	3.494	QY	•000						
W	•040	SX	335.519	MY	3.494	MX Y	•000	X	7.5	Y	7.5
W	•040	QX	•000	SY	335.519						
W	•030	MX	3.494	QY	•000						
W	•030	SX	335.519	MY	3.494	MX Y	•000	X	15.0	Y	15.0
W	•030	QX	•000	SY	335.519						
W	•000	MX	3.494	QY	•000						
W	•000	SX	335.519	MY	3.494	MX Y	•000	X	•0	Y	•0
W	•000	QX	•000	SY	335.519						

Table 30. Three Parameter Trigonometric Shape Function.

ALR	.044	BER	.044	GAR	-.027						
W	.062	MX	2.370	MY	3.754	MX Y	.000	X	.0	Y	.0
W	.062	SX	360.395	SY	360.395						
W	.062	QX	-.000	QY	-.000						
W	.057	MX	2.650	MY	4.757	MX Y	.000	X	7.5	Y	.0
W	.057	SX	321.445	SY	456.679						
W	.057	QX	.113	QY	-.000						
W	.044	MX	3.326	MY	7.178	MX Y	.000	X	15.0	Y	.0
W	.044	SX	227.413	SY	689.130						
W	.044	QX	.160	QY	-.000						
ALR	.044	BER	.044	GAR	-.027						
W	.062	MX	2.370	MY	3.754	MX Y	.000	X	.0	Y	.0
W	.062	SX	360.395	SY	360.395						
W	.062	QX	-.000	QY	-.000						
W	.049	MX	3.360	MY	3.854	MX Y	.000	X	7.5	Y	7.5
W	.049	SX	370.020	SY	370.020						
W	.049	QX	-.075	QY	-.075						
W	.000	MX	.000	MY	.000	MX Y	.000	X	15.0	Y	15.0
W	.000	SX	.000	SY	.000						
W	.000	QX	-.751	QY	-.751						

Table 31. Three Parameter Trigonometric Shape Function.

ALC	.035	BEC	.035	GAC	-.023				
W	.048	MX	4.147	MY	2.159	MX Y	.000	X	.0
W	.048	SX	207.289	SY	207.289				.0
W	.048	QX	.000	QY	.000				
W	.045	MX	3.899	MY	2.912	MX Y	.000	X	7.5
W	.045	SX	231.152	SY	279.599				.0
W	.045	QX	.200	QY	.000				
W	.035	MX	3.153	MY	5.172	MX Y	.000	X	15.0
W	.035	SX	302.739	SY	496.530				.0
W	.035	QX	.401	QY	.000				
ALC	.035	BEC	.035	GAC	-.023				
W	.048	MX	4.147	MY	2.159	MX Y	.000	X	.0
W	.048	SX	207.289	SY	207.289				.0
W	.048	QX	.000	QY	.000				
W	.040	MX	4.652	MY	3.161	MX Y	-.1.009	X	7.5
W	.040	SX	303.462	SY	303.462				7.5
W	.040	QX	.200	QY	.200				
W	.000	MX	6.166	MY	6.166	MX Y	-.4.037	X	15.0
W	.000	SX	591.980	SY	591.980				15.0
W	.000	QX	.401	QY	.401				

Table 32. Three Parameter Polynomial
Shape Function.

```

2 PROCEDURE RAT(QR1, QR2, QR3, A, B, L) $
2 BEGIN $
2 P = 3.1415927 $
2 E = 1**7 $
2 H = (0.25) $
2 N = (0.33) $
2 D = ((E(H*3)) / ((12.0)((1.0) - N*2))) $
2 ALRD=((2.0)((P*2)((A*2) + (B*2))*2))
2      - ((8.0) (((A*2) + N(B*2))*2))) QR1)
2      / ( (P*6) (A*2) (B*6) D ))
2      +((16.0)((B*2) + N(A*2)) ((A*2) + N(B*2)))
2      - (N(((A*2) + (B*2))*2))) QR2)
2      / ((P*6) (A*4) (B*4) D))
2      + ((8.0) (((8.0) N ((A*2) + N(B*2)))
2      - ((P*2)((B*2) + N(A*2))))(QR3))
2      / ( (P*7) (A*2) (B*4) D)) $
2 BERD=((16.0)((A*2) + N(B*2))((B*2) +
2      (N(A*2))) - (N(((A*2) + (B*2))*2)))QR1)
2      / ((P*6) (A*4) (B*4) D))
2      +((2.0)((P*2) (((A*2) + (B*2))*2)
2      - (8.0) (((B*2) + (A*2) N)*2))) QR2)
2      / ( (P*6) (A*6) (B*2) D)
2      +((8.0)((8.0) N ((B*2) + N(A*2))
2      - (P*2) ((A*2) + N(B*2))) QR3)
2      / ( (P*7) (A*4) (B*2) D)) $
2 GARD=((8.0)((8.0) N ((A*2) + N (B*2)))
2      - (P*2) ((B*2) + (A*2) N)) QR1)
2      / ( (P*7)(A*2)(B*4)D))
2      +((8.0)((8.0) N ((B*2) + N(A*2)))
2      - (P*2) ((A*2) + N(B*2))) QR2)
2      / ( (P*7) (A*4) (B*2) D))
2      +((4.0)((P*4) - (64.0) (N*2)) QR3)
2      / ( (P*8)(A*2) (B*2)D)) $
2 DET = (((P*4) (((A*2) + (B*2))*2))

```

```

2      + (((128.0) N ((A*2) + N(B*2))((B*2) + N(A*2)))
2      - ((8.0) (P*2) (((A*2) + N(B*2))*2))
2      - ((8.0) (P*2)((B*2) + N(A*2))*2))
2      - ((64.0) (N*2) (((A*2) + (B*2))*2)))
2      /(((16.0)(P*4)(A*5)(B*5)))
2 ALR      = ALRD / DET
2 BER      = BERD / DET
2 GAR      = GARD / DET
2 WRITE ($$OUT1, FMT1)
2 OUTPUT OUT1(ALR, BER, GAR)
2 FORMAT FMT1(*ALR*, X5.3, B5, *BER*, X7.3, B5, *GAR* , X7.3, W2)
2 FOR X = ( 0.0, 7.5, 15.0)
2 BEGIN
2 Y      = L.X
2 C      = COS((P.X) / ((2.0) A))
2 J      = COS((P.Y)/((2.0)B))
2 WM      = ALR.C + BER.J + GAR.J.C
2 MXM      = (((P*2)D) / ((4.0)(A*2)(B*2)))
2          (ALR (B*2).C ) + (BER.N.J.(A*2)
2          + (GAR (N(A*2) + (B*2))(J.C)))
2 MYM      = (((P*2)D) / ((4.0)(A*2)(B*2)))
2          ((ALR (B*2).N.C) + (BER.(A*2).J)
2          +(GAR ((A*2) + N (B*2))(J.C)))
2 MXYM      = (((GAC) (P*2) D. ((1.0) - N) (SIN((P.X)/((2.0)A)))
2          (SIN((P.Y) / ((2.0)B)))) / (( 4.0)(A.B)))
2 QXM      = (-1.0)((P*3)D) / ((8.0)(A*3)(B*2))
2          (SIN((P.X) / ((2.0)A)))
2          (ALR (B*2) + (GAR ((A*2) + (B*2)).(J)))
2 QYM      = (-1.0)((P*3)D) / ((8.0)(A*2)(B*3))
2          (SIN((P.Y) / ((2.0)B)))
2          (BER (A*2) +(GAR ((A*2)+(B*2) ).C))
2 SXM      = (((3.0)(P*2)D) / ((2.0).(A*2)(B*2)(H*2)))
2          (ALR (B*2).C + (BER.N.J (A*2))
2          + GAR ((B*2 + N(A*2))(J.C)))

```


2 END \$
2 END \$
2 FINISH \$

```

2 PROCEDURE MOUSE (QM1, QM2, A, B, L) $
2 BEGIN
2 P      = 3.1415927 $
2 E      = 1**7 $
2 H      = (0.25) $
2 N      = (0.33) $
2 D      = ((E (H*3)) / ((12.0)((1.0) - N*2))) $
2 ALR    = (((P*2)A) / (B((P*4) - (64.0)(N*2))))
2        (((32.0)(A*2)(QM1)) / ((P*2)D))
2        - (((256.0) N (B*2)(QM2)) / ((P*4) D))) $
2 BER    = (((P*2)B) / (A((P*4) - (64.0)(N*2))))
2        (((32.0) (B*2) QM2) / ((P*2) D))
2        - (((256.0) N (A*2).QM1) / (D(P*4)))) $
2 WRITE  ($$OUT1, FMT1) $
2 OUTPUT OUT1(ALR, BER) $
2 FORMAT FMT1(*ALR*, X5.3, B5, *BER*, X7.3, W2) $
2 FOR X = (0.0, 7.5, 15.0) $
2 BEGIN
2 Y      = L.X $
2 GAR    = 0 $
2 C      = COS((P.X) / ((2.0) A)) $
2 J      = COS((P.Y)/((2.0)B)) $
2 WM     = ALR.C + BER.J + GAR.J.C $
2 MXM    = (((P*2)D) / ((4.0)(A*2)(B*2)))
2        (ALR (B*2).C ) + (BER.N.J.(A*2)
2        + (GAR (N(A*2) + (B*2))(J.C))) $
2 MYM    = (((P*2)D) / ((4.0)(A*2)(B*2)))
2        ((ALR (B*2).N.C) + (BER.(A*2).J)
2        + (GAR ((A*2) + N (B*2))(J.C))) $
2 MYM    = (((GAC) (P*2) D. ((1.0) - N) (SIN((P.X)/((2.0)A)))
2        (SIN((P.Y) / ((2.0)B)))) / (( 4.0)(A.B))) $
2 QXM    = (-1.0)((P*3)D) / ((8.0)(A*3)(B*2))
2        (SIN((P.X) / ((2.0)A)))
2        (ALR (B*2) + (GAR ((A*2) + (B*2)).(J))) $

```

```

2 QYM      = ((-1.0)((P*3)D) / ((8.0)(A*2)(B*3)))
2           (SIN((P.Y) / ((2.0)B)))
2           (BER (A*2) + (GAR ((A*2) + (B*2) ).C))
2 SXM      = (((3.0)(P*2)D) / ((2.0).(A*2)(B*2)(H*2)))
2           (ALR (B*2).C + (BER.N.J (A*2))
2           + GAR ((B*2 + N(A*2))(J.C)))
2 SYM      = (((3.0)(P*2)D) / ((2.0)(A*2)(B*2)(H*2)))
2           ((ALR.N.(B*2).C + BER.(A*2).J)
2           + GAR ((A*2) + N.(B*2))(J.C))
2 WRITE    ($$OUT2, FMT2)
2 WRITE    ($$OUT3, FMT3)
2 WRITE($$OUT4, FMT4)
2 OUTPUT    OUT2(WM, MXM, MYM, MXYM ,X, Y)
2 OUTPUT    OUT3(WM, SXM, SYM)
2 OUTPUT    OUT4(WM, QXM, QYM)
2 FORMAT FMT2(*WM*,X6.3,B5, *MXM*, X8.3, B5, *MYM*, X8.3, B5,
2           *MXYM*, X7.3, B5, *X*, X6.1 , B5, *Y*, X6.1, W2)
2 FORMAT FMT3(*WM*, X6.3, B5, *SXM*, X8.3, B5, *SYM*, X8.3, W2)
2 FORMAT FMT4(*WM*, X6.3, B5, *QXM*, X8.3, B5, *QYM*, X8.3, W2)
2 END
2 RETURN
2 END
2 COMMENT
2 THE FOLLOWING COMPUTATIONS ARE FOR A DISTRIBUTED LOAD OVER THE
2 PLATE
2 Q      = (0.0466)
2 BEGIN
2 FOR L = (0,1,1)
2 BEGIN
2 A = (15.0)
2 BEGIN
2 B = A
2 P      = 3.1415927
2 QR1    = (((2.0)A.B.Q) / P)

```

```

2 QR2      =   QR1
2 QR3      =   (((4.0).Q.A.B )/ (P*2))
2 QM1      =   QR1
2 QM2      =   QR2
2 MOUSE(QM1, QM2, A, B, L)
2 END      $
2 END      $
2 END      $
2 FINISH   $

```

\$
\$
\$
\$
\$
\$

```

2 COMMENT
2 JOHN SIMONIS
2 STRESS AND DEFLECTION FOR A PLATE SUPPORTED AT
2 FOUR CORNERS
2
2 DEFINATION OF SYMBOLS
2 AL, BE, GA ARE THE VARIABLE COEFFICIENTS
2 W IS DEFLECTION
2 MX, MY, MXY IS THE MOMENT
2 QX, QY ARE THE SHEAR
2 SX, SY ARE THE STRESSES
2 REST OF THE SYMBOLS ARE AS DEFINED IN THE THESIS
2 PROCEDURE DOG(QD1, QD2, A, B, L)
2 BEGIN
2 E      = 1**7
2 H      = (0.25)
2 N      = (0.33)
2 D      = ((E (H*3)) / ((12.0) ((1.0) - N*2)))
2 ALD    = ((A ((A*2) QD1) - (N (B*2) QD2)))
2        / ((4.0).B.D.((1.0) - (N*2)))
2 BED    = ((B ((B*2) QD2) - (N (A*2) QD1)))
2        / ((4.0).A.D.((1.0) - (N*2)))
2 WRITE ($$OUT1, FMT1)
2 OUTPUT OUT1(ALD, BED)
2 FORMAT FMT1(*ALD*, X5.3, B5, *BED*, X7.3, W2)
2 FOR X = (0.0, 7.5, 15.0)
2 BEGIN
2 Y = L.X
2 ALC    = ALD
2 BEC    = BED
2 GAC    = (0.0)
2 AX     = ((A*2) - (X*2))
2 BY     = ((B*2) - (Y*2))
2 WD     = (((ALC (AX)) / (A*2)) + ((BEC (BY)) / (B*2))

```

```

2      +(GAC (AX) (BY)) / (A*2)(B*2))      $
2 MXD      = (( (2.0) D) / (A*2)(B*2))(ALC(B*2)
2      +(BEC.N.(A*2) + (BY -(N.AX)) GAC))      $
2 MYD      = (( (2.0) D) / (A*2)(B*2))(ALC.N.(B*2)
2      +(BEC.(A*2) + (N(BY) +(AX)) GAC))      $
2 MXYD     = (( (4.0).D.X.Y.GAC ((1.0) - N) / (A*2)(B*2))
2      $
2 QXD      = (( (-1.0)(4.0).D.X.GAC) / (A*2)(B*2))
2      $
2 QYD      = (( (-1.0)(4.0).D.Y.GAC) / (A*2)(B*2))
2      $
2 SXD      = ((( (12.0) D) / ((A*2)(B*2)(H*2)))
2      (ALC (B*2) + BEC . N.(A*2) +
2      ((BY) + N(AX)) GAC))      $
2 SYD      = ((( (12.0) D) / ((A*2)(B*2)(H*2)))
2      (ALC.N.(B*2) + (BEC)(A*2) +
2      (N(BY) + (AX)) GAC))      $
2 WRITE ($$OUT2, FMT2)      $
2 WRITE ($$OUT3, FMT3)      $
2 WRITE($$OUT4, FMT4)      $
2 OUTPUT OUT2(WD, MXD, MYD, MXYD, X, Y)      $
2 OUTPUT OUT3(WD, SXD, SYD)      $
2 OUTPUT OUT4(WD, QXD, QYD)      $
2 FORMAT FMT2(*WD*,X6.3,B5, *MXD*, X8.3, B5, *MYD*, X8.3, B5,
2      *MXYD*, X7.3, B5, *X*, X6.1, B5, *Y*, X6.1, W2)      $
2 FORMAT FMT3(*WD*, X6.3, B5, *SXD*, X8.3, B5, *SYD*, X8.3, W2)      $
2 FORMAT FMT4(*WD*, X6.3, B5, *QXD*, X8.3, B5, *QYD*, X8.3, W2)      $
2 END      $
2 RETURN      $
2 END      $
2 COMMENT
2 THE FOLLOWING COMPUTATIONS ARE FOR A DISTRIBUTED LOAD OVER THE
2 PLATE      $
2 Q      = (0.0466)      $
2 BEGIN
2 A = (15.0)      $
2 BEGIN

```


2 FOR L = (0,1,1)	\$
2 BEGIN	
2 B = A	\$
2 QC1 = (Q.A.B.(2.0) / (3.0))	\$
2 QC2 = QC1	\$
2 QC3 = (Q.A.B (4.0) / (9.0))	\$
2 QD1 = QC1	\$
2 QD2 = QC2	\$
2 DOG(QD1, QD2, A, B, L)	\$
2 END	\$
2 END	\$
2 END	\$
2 FINISH	\$

```

2 PROCEDURE CAT(QC1, QC2, QC3, L, A, B) $
2 BEGIN
2 E = 1**7 $
2 H = (0.25) $
2 N = (0.33) $
2 D = (E (H*3) / ((12.0) ((1.0) - N*2))) $
2 ALCD = (((A*3) B) / ((30.0) D))
2      (((A*2)((A*4) + (B*4) ((6.0) - (5.0)(N*2))
2      + ((10.0) (A*2) (B*2) ((1.0) - N))) QC1)
2      + ((B*2) ((5.0)(A*2)(B*2) + (5.0)(N*2)(A*2)(B*2)
2      - N(B*4) - N(A*4) - (10.0)(N)(A*2)(B*2)) QC2)
2      + ((7.5)(A*2)(B*4) ((N*2) - (1.0)) QC3 )) $
2 BECD = (A(B*3) / ((30.0) D)) (
2      ((A*2) ((5.0)(A*2)(B*2) - N(A*4) - N(B*4)
2      + (5.0)(N*2)(A*2)(B*2) - (10.0)(N)(A*2)(B*2)) QC1)
2      + ((B*2) ((B*4) + (A*4) ((6.0) - (5.0) (N*2))
2      + (10.0)(A*2)(B*2) ((1.0) - N)) QC2)
2      + ((7.5)(A*4)(B*2) ((N*2) - (1.0)) QC3)) $
2 GACD = (((A*5)(B*5)((N*2) - (1.0)) / ((4.0) D))
2      (QC1 + QC2 - (1.5) QC3)) $
2 DET = ( (2.0)(A*2)(B*2) (((1.0) - N*2))
2      (((10.0)(A*2)(B*2)((1.0) - N)) + (A*4)
2      + (B*4)) / (15.0)) $
2 ALC = ALCD / DET $
2 BEC = BECD / DET $
2 GAC = GACD / DET $
2 WRITE ($$OUT1, FMT1) $
2 OUTPUT OUT1(ALC, BEC, GAC) $
2 FORMAT FMT1(*ALC*, X5.3, B5, * BEC*, X7.3, B5, *GAC*, X7.3, W2) $
2 FOR X = (0.0, 7.5, 15.0) $
2 BEGIN
2 Y = L.X $
2 AX = ((A*2) - (X*2)) $
2 BY = ((B*2) - (Y*2)) $

```

```

2 WD      = ((( ALC (AX)) / (A*2)) + ((BEC (BY)) / (B*2))
2          + (GAC (AX) (BY)) / (A*2)(B*2))
2          $
2 MXD      = ((( 2.0) D) / (A*2)(B*2))(ALC(B*2)
2          + (BEC.N.(A*2) + (BY - (N.AX) ) GAC))
2          $
2 MYD      = (((2.0)D) / (A*2)(B*2))(ALC.N.(B*2)
2          + (BEC.(A*2) + (N(BY) + (AX)) GAC))
2          $
2 MXYD     = ((4.0).D.X.Y.GAC ((1.0) - N) / (A*2)(B*2))
2          $
2 QXD      = (((-1.0)(4.0).D.X.GAC) / (A*2)(B*2))
2          $
2 QYD      = (((-1.0)(4.0).D.Y.GAC) / (A*2)(B*2))
2          $
2 SXD      = (((12.0) D) / ((A*2)(B*2)(H*2)))
2          (ALC (B*2) + BEC . N.(A*2) +
2          (BY) + N(AX)) GAC))
2          $
2 SYD      = (((12.0)D) / ((A*2)(B*2)(H*2)))
2          (ALC.N.(B*2) + (BEC)(A*2) +
2          (N(BY) + (AX)) GAC))
2          $
2 WRITE ($$OUT2, FMT2)
2          $
2 WRITE ($$OUT3, FMT3)
2          $
2 WRITE($$OUT4, FMT4)
2          $
2 OUTPUT OUT2(WD, MXD, MYD, MXYD, X, Y)
2          $
2 OUTPUT OUT3(WD, SXD, SYD)
2          $
2 OUTPUT OUT4(WD, QXD, QYD)
2          $
2 FORMAT FMT2(*WD*,X6.3,B5, *MXD*, X8.3, B5, *MYD*, X8.3, B5,
2          *MXYD*, X7.3, B5, *X*, X6.1 , B5, *Y*, X6.1, W2)
2          $
2 FORMAT FMT3(*WD*, X6.3, B5, *SXD*, X8.3, B5, *SYD*, X8.3, W2)
2          $
2 FORMAT FMT4(*WD*, X6.3, B5, *QXD*, X8.3, B5, *QYD*, X8.3, W2)
2          $
2 END
2          $
2 RETURN
2          $
2 END
2          $
2 COMMENT
2 THE FOLLOWING COMPUTATIONS ARE FOR A DISTRIBUTED LOAD OVER THE
2 PLATE
2          $
2 Q      = (0.0466)
2          $
2 BEGIN
2          $
2 FOR L = (0,1,1)
2          $

```

```

2 BEGIN
2 A = (15.0)      $
2 BEGIN
2 B = A      $
2 QC1      =      (Q.A.B.(2.0) / (3.0))
2 QC2      =      QC1
2 QC3      =      (Q.A.B (4.0) / (9.0))
2 QD1      =      QC1
2 QD2      =      QC2
2 CAT(QC1, QC2, QC3, L, A, B)
2 END
2 END
2 END
2 FINISH

```

```

$
$
$
$
$
$
$
$
$

```

```

2 COMMENT
2 PRINCIPAL STRESS USING AN EQUILIBRIUM STRAIN ROSETTE
2 JOHN SIMONIS
2 THE STRAIN ROSETTE HAS EA LOCATED AT AN ANGLE
2 OF PI FROM THE PRINCIPAL AXIS
2 EB IS 60 DEGREES FROM EA
2 EC IS 120 DEGREES FROM EA
2 E IS THE MODULUS OF ELASTICITY
2 G IS THE SHEAR MODULUS PF ELASTICITY
2 N IS POISSON RATIO
2 S1 IS THE PRINCIPAL STRESS
2 S2 IS THE SECOND PRINCIPAL STRESS
2 TM IS THE MAX SHEAR STRESS
2 PHI IS THE ANGLE EA MAKES WITH THE PRINCIPAL STRESS $
2 INPUT DATA (EA1, EB1, EC1) $
2 START..
2 BEGIN
2 READ ($$DATA) $
2 N = (0.33) $
2 E = (10.0) $
2 G = E/((2.0)((1.0) + N)) $
2 EA = EA1(2.0)/(2.09) $
2 EB = EB1(2.0)/(2.09) $
2 EC = EC1(2.0)/(2.09) $
2 S1 = E((EA+EB+EC)/(3.0)((1.0)-N)+
2 (SQRT((EA-((EA+EB+EC)/(3.0)))^2 +
2 ((EC-EB)^2/(3.0))))/((1.0) + N))) $
2 S2 = E((EA+EB+EC)/(3.0)((1.0)-N)-
2 (SQRT((EA-((EA+EB+EC)/(3.0)))^2 +
2 ((EC-EB)^2/(3.0))))/((1.0) + N))) $
2 TM = G.(2.0).SQRT((EA-((EA+EB+EC)/(3.0)))^2
2 + ((EC-EB)^2/(3.0))) $
2 PHI = (0.5) ARCTAN(((EC-EB)/SQRT(3.0)) /
2 (EA - ((EA+EB+EC)/(3.0)))) $

```

```
2 WRITE ($$OUT, ANS) $
2 END $
2 GO TO START $
2 OUTPUT OUT(EA, EB, EC, E, N, S1, S2, TM, PHI) $
2 FORMAT ANS(9X11.5, W4) $
2 FORMAT TITLE(B4,*EA*,B10,*EB*,B10,*EC*,B11,
2 *E*,B11*N*,B10,*S1*,B10*S2*,B10,*TM*,B10,*PHI*, W2) $
2 FINISH $
```

BIBLIOGRAPHY

1. Courant, R., Calculus of Variations and Supplementary Notes and Exercises, New York University, 1956-1957.
2. Hetenyi, M. (Ed.), Handbook of Experimental Stress Analysis, John Wiley and Sons, 1950.
3. Courant, R., "Variational Methods for the Solution of Problems of Equilibrium and Vibrations," American Mathematical Society Bulletin, Vol. 49, 1943, p. 1-23.
4. Hilderbrand, F. B., Methods of Applied Mathematics, Prentice-Hall, 1961.
5. Hodgeman, C. D. (ed.), C.R.C. Standard Mathematical Tables, Chemical Rubber Publishing Company.
6. Hradek, R. W., Uniformly Loaded Square Plates which are Simply Supported at the Four Corners, Thesis submitted at University of Iowa, February, 1958.
7. Langhaar, H. L., Energy Methods in Applied Mechanics, John Wiley and Sons, 1962.
8. Love, A.E.H., A Treatise on the Mathematical Theory of Elasticity, Dover Publications, 1944.
9. Lee, G. H., An Introduction to Experimental Stress Analysis, John Wiley and Sons, 1950.
10. Lee, S. L. and P. Ballesteros, "Uniformly Loaded Rectangular Plates Supported at the Corners," International Journal of Mechanical Science, Vol. 2, 1960, p. 206-211.
11. Oden, J. T., "Analysis of Thin Plates Supported at Their Corners," Ph.D. Report Oklahoma State University, 1963.
12. Perry, C. C. and H. R. Lissner, The Strain Gage Primer, McGraw-Hill, 1962.
13. Sagan, Hans, Boundary and Eigenvalue Problems in Mathematical Physics, John Wiley and Sons, 1961.
14. Temple, G. and W. G. Beckley, Rayleigh's Principle, Dover Publications, 1956.

15. Timoshenko, S. and J. N. Goodier, Theory of Elasticity, McGraw-Hill, 1951.
16. Timoshenko, S. and S. Woinowsky-Krieger, Theory of Plates and Shells, John Wiley and Sons, 1959.
17. Trefftz, E., "Konvergenz beweis für einen Spezialfall," Handbuch der Physik, Vol. 6, 1928, p. 132-137.
18. Wang, Chi Leh, Applied Elasticity, McGraw-Hill, 1953.
19. Weed, N. R. and W. L. Davis, Fundamentals of Electronic Devices and Circuits, Prentice-Hall, 1959.
20. Wylie, Jr., C. R., Advanced Engineering Mathematics, McGraw-Hill, 1960.